

# Towards universal topological quantum computation in the $\nu = \frac{5}{2}$ fractional quantum Hall state

Michael Freedman,<sup>1</sup> Chetan Nayak,<sup>1,2</sup> and Kevin Walker<sup>1</sup>

<sup>1</sup>*Microsoft Research, Project Q, Kohn Hall, University of California, Santa Barbara, California 93108, USA*

<sup>2</sup>*Department of Physics and Astronomy, University of California, Los Angeles, California 90095-1547, USA*

(Received 28 January 2006; published 7 June 2006)

The Pfaffian state, which may describe the quantized Hall plateau observed at Landau level filling fraction  $\nu = \frac{5}{2}$ , can support topologically-protected qubits with extremely low error rates. Braiding operations also allow perfect implementation of certain unitary transformations of these qubits. However, in the case of the Pfaffian state, this set of unitary operations is not quite sufficient for universal quantum computation (i.e. is not dense in the unitary group). If some topologically unprotected operations are also used, then the Pfaffian state supports universal quantum computation, albeit with some operations which require error correction. On the other hand, if certain topology-changing operations can be implemented, then fully topologically-protected universal quantum computation is possible. In order to accomplish this, it is necessary to measure the interference between quasiparticle trajectories which encircle other moving trajectories in a time-dependent Hall droplet geometry [cond-mat/0512072].

DOI: [10.1103/PhysRevB.73.245307](https://doi.org/10.1103/PhysRevB.73.245307)

PACS number(s): 73.43.Fj, 03.67.Lx, 03.67.Mn, 03.67.Pp

## I. INTRODUCTION

The fractional quantum Hall regime<sup>2</sup> contains a cornucopia of Abelian fractional quantum Hall states, i.e., states whose quasiparticle excitations have Abelian braiding statistics.<sup>3,4</sup> It is possible that an even more wonderful phenomenon may occur there: non-Abelian quantum Hall states. The strongest candidate is the  $\nu = \frac{5}{2}$  quantum Hall state. This state is quite robust in the highest-mobility samples,<sup>5</sup> and numerical studies indicate that the Pfaffian state,<sup>6,7</sup> which has excitations exhibiting non-Abelian braiding statistics,<sup>8–16</sup> has large overlap with the exact ground state for small numbers of electrons at this filling fraction.<sup>17,18</sup> An experiment has been proposed<sup>19</sup> which would determine if the  $\nu = \frac{5}{2}$  state is, indeed, in the universality class of the Pfaffian state by observing the signature of non-Abelian statistics: a degenerate set of multi-quasiparticle states that cannot be distinguished locally but can be distinguished by a non-Abelian analog of the Aharonov-Bohm interference measurement. In the two quasiparticle case, this is simply the observation of a topologically-protected qubit.<sup>20,21</sup> In the presence of many pairs of quasiparticles, all kept far apart, the topologically degenerate ground states form many qubits. These states are locally indistinguishable. If the environment interacts only locally with the system, it cannot act on these qubits. Braiding the quasiparticles around each other, an intrinsically non-local operation, transforms the qubits. These gates are exact because small deformations of the quasiparticle trajectories do not affect their braiding topology. However, there is a sense in which the Pfaffian state is not quite non-Abelian enough: the set of all possible braiding operations only gives a finite set of unitary transformations on the qubits. Thus, with these operations, it is not possible to perform any desired unitary transformation, which would be necessary for a universal quantum computer.

In this paper, we suggest ways in which this apparent shortcoming of the Pfaffian state (and, by implication, the  $\nu = \frac{5}{2}$  quantum Hall state) can be circumvented.<sup>1</sup> The first, more pedestrian, approach is to use some nontopological operations. Consider, for instance, what happens when two qua-

siparticles are brought close together. The degeneracy between the two states of their qubit is broken. Since unitary evolution in time will now cause a phase difference to develop between the two states of the qubit, we thereby implement a phase gate. We explain how a universal quantum computer can be constructed using these ideas. The second, more interesting, approach relies on (1) the construction by Bravyi and Kitaev<sup>22</sup> of a universal set of gates for the Pfaffian state that exploits topology change in an abstract context in which there are no restrictions on the global topology of spacetime (using, for instance, overcrossings and undercrossings, which seem unlikely to be realized in a system of electrons confined to a plane); and (2) the observation that their operations actually *can* be implemented in a way that remains entirely in the plane as long as one is able to measure the interference between trajectories encircling quasiparticles that are moving, merging, and splitting—i.e., interference in a time-dependent background Hall fluid. We note, in passing, that  $\nu = \frac{12}{5}$  may also be a non-Abelian state, specifically one of the states proposed by Read and Rezayi.<sup>23</sup> It may be particularly interesting—even though it is seen more weakly—because, if it is indeed a Read-Rezayi state,<sup>23</sup> braiding operations alone are sufficient to implement any unitary transformation to within a desired accuracy—i.e., it supports topologically protected universal quantum computation.<sup>24</sup> In the event that the  $\nu = \frac{12}{5}$  state proves to be simply an Abelian state or to have too small an energy gap to permit manipulation, the protocols described in this paper, if they can be experimentally realized, would save the day by boosting the computational power of the  $\nu = \frac{5}{2}$  state so that it, too, can be regarded as a universal quantum computer. Furthermore, the basic architecture that we describe in Secs. II and III is relevant to the  $\nu = \frac{12}{5}$  state as well.

## II. QUBITS IN THE PFAFFIAN STATE

In this paper, we will assume that the  $\nu = \frac{5}{2}$  plateau is in the universality class of the Pfaffian quantum Hall state. In this section, we list some basic facts about the Pfaffian quan-

tum Hall state and introduce some notation that will be useful in the following sections. The goal is to describe the qubits that arise when many quasiparticles<sup>25</sup> are present.

The Pfaffian wave function<sup>6,7</sup> takes the form

$$\Psi_{\text{g.s.}}(z_j) = \prod_{j<k} (z_j - z_k)^2 \prod_j e^{-|z_j|^2/4} \cdot \text{Pf} \left( \frac{1}{z_j - z_k} \right), \quad (1)$$

where the Pfaffian is the square root of the determinant of an antisymmetric matrix. It has a Landau level filling factor  $1/2$ . (There is an obvious generalization to other even filling factors and also to odd filling factors of bosonic particles.) It does not appear to be a good description of electrons at filling fraction  $1/2$ , which are in a metallic state down to the lowest observable temperatures (see Ref. 2 and references therein). However, it is a candidate for the half-filled first excited Landau level of the observed  $\nu = \frac{5}{2} = 2 + \frac{1}{2}$  quantum hall plateau.<sup>5</sup> If we assume that the filled lowest Landau level of both spins is inert and translate the Pfaffian wave function to the first excited Landau level, it has high overlap with the exact ground state wave function of small systems of electrons interacting through Coulomb interactions in a half-filled first excited Landau level.<sup>17,18</sup> The Pfaffian state is also the exact ground state of a certain three-body Hamiltonian.<sup>7</sup> While this three-body Hamiltonian is unrealistic, it has the advantage that we can also write down exact multi-quasihole wave functions. Since it appears from numerical studies of small systems that this three-body Hamiltonian is in the same universality class as the actual Hamiltonian of the real sys-

tem, we will assume that these multi-quasihole states capture the essential topological features of the excitations of the  $\nu = \frac{5}{2}$  quantum Hall state.

The form of the Pfaffian factor in this wave function,

$$\text{Pf} \left( \frac{1}{z_j - z_k} \right) = \mathcal{A} \left( \frac{1}{z_1 - z_2} \frac{1}{z_3 - z_4} \dots \right) \quad (2)$$

is strongly reminiscent of the real-space form of the BCS wave function. Indeed, the Pfaffian state may be viewed as a quantum Hall state of  $p$ -wave paired fermions.<sup>12-14</sup>

The fundamental quasiparticles in this state carry half of a flux quantum and, therefore, charge  $e/4$ . A wave function for a two-quasihole state may be written as follows:

$$\Psi_{\text{g.s.}}(z_j) = \prod_{j<k} (z_j - z_k)^2 \prod_j e^{-|z_j|^2/4} \times \text{Pf} \left( \frac{(z_j - \eta_1)(z_k - \eta_2) + z_j \leftrightarrow z_k}{z_j - z_k} \right). \quad (3)$$

When the two quasiholes at  $\eta_1$  and  $\eta_2$  are brought together at the point  $\eta$ , a single flux quantum quasiparticle results:

$$\Psi_{\text{g.s.}}(z_j) = \prod_{j<k} (z_j - z_k)^2 \prod_j e^{-|z_j|^2/4} \times \prod_i (z_i - \eta) \text{Pf} \left( \frac{1}{z_j - z_k} \right). \quad (4)$$

The situation becomes more interesting when we consider states with four quasiholes. A wave function with four quasiholes at  $\eta_1, \eta_2, \eta_3, \eta_4$  takes the form

$$\Psi_{(13)(24)}(z_j) = \prod_{j<k} (z_j - z_k)^2 \prod_j e^{-|z_j|^2/4} \times \text{Pf} \left( \frac{(z_j - \eta_1)(z_j - \eta_3)(z_k - \eta_2)(z_k - \eta_4) + (j \leftrightarrow k)}{z_j - z_k} \right). \quad (5)$$

However, there is another wave function with four quasiholes at  $\eta_1, \eta_2, \eta_3, \eta_4$ :

$$\Psi_{(14)(23)}(z_j) = \prod_{j<k} (z_j - z_k)^2 \prod_j e^{-|z_j|^2/4} \times \text{Pf} \left( \frac{(z_j - \eta_1)(z_j - \eta_4)(z_k - \eta_2)(z_k - \eta_3) + (j \leftrightarrow k)}{z_j - z_k} \right). \quad (6)$$

These two wave functions are linearly independent, but they have the same charge density profiles as long as  $\eta_1, \eta_2, \eta_3, \eta_4$  are far apart. In fact, they are indistinguishable by any local measurement. One might even think that there is a third four-quasihole state  $\Psi_{(12)(34)}$ , but this is not independent of the other two,<sup>8</sup>

$$\Psi_{(14)(23)} - \Psi_{(12)(34)} = x(\Psi_{(13)(24)} - \Psi_{(12)(34)}) \quad (7)$$

where  $x = (\eta_1 - \eta_3)(\eta_2 - \eta_4) / (\eta_1 - \eta_4)(\eta_2 - \eta_3)$ .

It is enlightening to pick as the basis of the two dimensional space of four-quasihole wave functions  $\Psi_{(13)(24)}$  and the following state<sup>11</sup> ( $\mathcal{N}$  is a normalization factor):

$$\Psi_{(13)(24)} - \Psi_{(14)(23)} = \mathcal{N} \prod_{j<k} (z_j - z_k)^2 \prod_j e^{-|z_j|^2/4} \times \mathcal{A} \left( \frac{z_1^0 z_1^1 (z_3 - \eta_1)(z_3 - \eta_3)(z_4 - \eta_2)(z_4 - \eta_4) (z_5 - \eta_1)(z_5 - \eta_3)(z_4 - \eta_2)(z_6 - \eta_4)}{z_1 z_2 \dots z_3 - z_4 \dots z_5 - z_6} \dots \right). \quad (8)$$

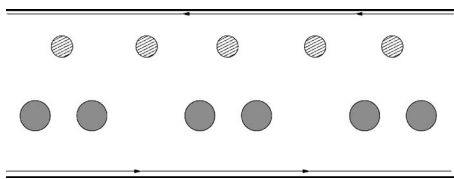


FIG. 1. A system with  $n$  quasihole pairs (held at pairs of antidots, depicted as shaded circles) supports  $n$  qubits. Additional antidots (hatched) can be used to move the quasiparticles, as described in Sec. III.

The interpretation is that a Cooper pair can be broken and the resulting neutral fermions put into zero modes.<sup>11</sup> In this case, the zero modes have wave functions  $z^0$  and  $z^1$ ; in the  $n$ -quasihole case, they have the form  $z^k$  with  $0 \leq k \leq n-1$ . In fact, a Cooper pair can even be broken when there are only two quasiparticles, but only one of the neutral fermions can go into a bulk zero mode; the other one must be at the edge. (Similarly, in the four-quasihole case, there are two additional states in which a neutral fermion is in one of the two zero modes while the other one is at the edge.)

In this way, it can be seen that there are  $2^n$   $2n$ -quasihole states<sup>8,11</sup> (half of them have a neutral fermion at the edge and the other half do not). It has been shown<sup>12</sup> that precisely the same degeneracy is obtained in a  $p+ip$  superconductor when there are  $2n$  flux  $hc/2e$  vortices present: there is one zero mode solution of the Bogoliubov-de Gennes equations per vortex. These solutions are Majorana modes. Grouping them into pairs, we have  $n$  fermionic levels, each of which can be occupied or unoccupied. By breaking Cooper pairs, we can change their occupancies. *We interpret this degeneracy as  $n$  qubits, one qubit for each pair of quasiholes.* (Of course, the grouping of quasiholes into pairs is arbitrary and any two pairings are related by the  $a$  change of basis.)

Hence, we envision a platform for quantum computation depicted in Fig. 1. An  $n$ -qubit system can be created by endowing a Hall bar with  $2n$  antidots at which quasiholes are pinned. Each pair of quasiholes has a two-dimensional Hilbert space spanned by  $|0\rangle$  and  $|1\rangle$ , which correspond to the absence or presence of a neutral fermion. In the following sections, we will discuss how these qubits can be manipulated and measured.

These qubits will be manipulated by braiding quasiparticles, which causes states in this  $2^n$ -dimensional Hilbert space to transform into each other. To discuss these transformations, a different basis than (5) is useful. The effect of braiding quasiparticles is a combination of the explicit monodromy of the wave function and the Berry matrices obtained from adiabatic transport of the  $\eta_i$ 's. The phase factors in (9) below have been chosen so that the latter are trivial and the former completely encapsulate quasiparticle braiding properties.<sup>8</sup> (We could have worked with the basis  $\Psi_{(13)(24)}$ ,  $\Psi_{(14)(23)}$ , in which there is no explicit monodromy, but then we would have to evaluate Berry matrix integrals.<sup>9,10</sup>)

$$\Psi^{(0,1)}(z_j) = \frac{(\eta_{13}\eta_{24})^{1/4}}{(1 \pm \sqrt{x})^{1/2}} (\Psi_{(13)(24)} \pm \sqrt{x}\Psi_{(14)(23)}), \quad (9)$$

where  $\eta_{13} = \eta_1 - \eta_3$ , etc. and  $x = \eta_{14}\eta_{23}/\eta_{13}\eta_{24}$ . [Note that we have taken a slightly different anharmonic ratio  $x$  than in

Ref. 8 in order to make (9) more compact than Eqs. (7.17), (7.18) of Ref. 8.] From this expression, we see, for instance, that taking  $\eta_3$  around  $\eta_1$  transforms  $\Psi^{(0)}(z_j)$  into  $\Psi^{(1)}(z_j)$ .

In the  $2n$ -quasihole case, the result can be stated as follows.<sup>8,13</sup> The  $2^n$  states of the system can be grouped into a representation of the Clifford algebra

$$\{\gamma_i, \gamma_j\} = 2\delta_{ij}, \quad (10)$$

with  $i, j = 1, 2, \dots, 2n$ . We could, for instance, organize the states according to their eigenvalues  $\psi_i^\dagger \psi_i = \pm 1$ , where  $\psi_j = \gamma_{2j-1} + i\gamma_{2j}$ ,  $j = 1, 2, \dots, n$ . When quasiparticles  $i$  and  $j$  are exchanged, the states transform according to:<sup>8,13</sup>

$$|\Psi\rangle \rightarrow e^{-(\pi/4)\gamma_i\gamma_j}|\Psi\rangle. \quad (11)$$

These braiding matrices,  $\tau_{ij} = \exp[-(\pi/4)\gamma_i\gamma_j]$  will be a set of topologically protected unitary transformations that we can use to manipulate our qubits.

Several important calculational and heuristic tools follow from field theories for the Pfaffian state. While they illuminate this section and Sec. III, they are somewhat technical and take us away from the main line of our exposition, so we have deferred a discussion of these field theories to Appendix A. For reasons that are discussed there, it is convenient to call excitations that have the same braiding properties (up to Abelian phase factors) as, respectively, (a) the vacuum, (b) charge- $e/4$  quasiparticles, and (c) neutral fermions either 1,  $\sigma$ ,  $\psi$  or, equivalently, isospin  $0, \frac{1}{2}, 1$ .

Thus far, we have assumed that the only quasiparticles in our system are the quasiparticles which we have induced on our antidots. There could also be thermally excited quasiparticles. They are the main source of error and their density was estimated in Ref. 19 to be exponentially small at low temperatures. However, even at zero temperature, there will always be some quasiparticles that are trapped by local variations in the potential, such as those caused by impurities. Assuming that they cannot move, the effect of these quasiparticles can always be accounted for with "software," i.e. quantum computations must be done with some more complicated algorithms that compensate for the presence of these stray quasiparticles. As a practical matter, however, we would like to make them as benign as possible. To the extent that we can tune the magnetic field to the center of the plateau and use gates to move the edge of the system to avoid impurities (as in Ref. 28), we should do so. If we can remove these localized quasiparticles with gates or a scanning probe microscope tip [such as an atomic-force microscope (AFM) tip] we should also attempt this. Finally, one simplifying feature of the Pfaffian state, in particular, noted in Refs. 28 and 29, is that there is an even-odd effect with quasiparticles. An even number of quasiparticles fuse to form a quasiparticle with Abelian statistics, while an odd number of quasiparticles fuse to form a quasiparticle with non-Abelian statistics. Hence, we handle stray localized quasiparticles in the following way. We should associate each stray quasiparticle with one of the antidots (most naturally the antidot to which it is closest). Then, we want the number of stray quasiparticles associated with each antidot to be even. In this way, the degrees of freedom of the antidot are not modified by its associates. Finally, we need to ensure that the quasiparticle

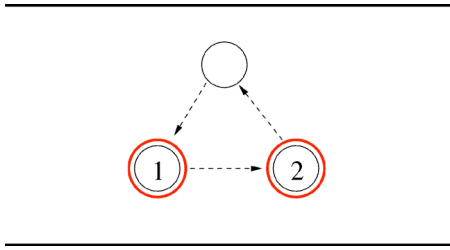


FIG. 2. (Color online) The exchange of two qubits through a third antidot.

braiding trajectories always encircle an even number of stray quasiparticles. Then, as may be seen from a repeated application of (11), the braiding matrices acting on the qubit Hilbert space are unaffected by the presence of the stray quasiparticles and the Hilbert space of the stray quasiparticles will not become entangled with it.

### III. BRAIDING AND INTERFEROMETRY

#### A. Braiding

The basic process by which we will manipulate many-quasiparticles states is the counterclockwise exchange depicted in Fig. 2. We suppose that the quasiparticles are localized at antidots and that they are transferred from one antidot to another by varying the voltages on the antidots. With three antidots, an exchange can be performed. Two successive exchanges results in a full braid of one quasiparticle around the other. We may need to move one quasiparticle greater distances—for instance, to take it around several others—in which case we could use an array of antidots as a “bucket brigade” (as in CCD devices such as digital cameras).

The process depicted in Fig. 2 can be used, for instance, to exchange a quasiparticle from one qubit with a quasiparticle from a different qubit. Such a process, which applies the gate  $g_3$  ( $g_1$  and  $g_2$  will be introduced later) has a spacetime diagram that is depicted later in Fig. 14:

$$g_3 = \frac{1}{\sqrt{2}} \begin{pmatrix} 1 & 0 & 0 & -i \\ 0 & 1 & -i & 0 \\ 0 & -i & 1 & 0 \\ -i & 0 & 0 & 1 \end{pmatrix}. \quad (12)$$

This will be one of the basic gates used below.

One can imagine another possibility, which might become realistic at some point in the future: one quasiparticle could be dragged around another with a scanning probe microscope tip, e.g., an AFM tip, which could couple to a quasiparticle electrostatically with the required spatial resolution

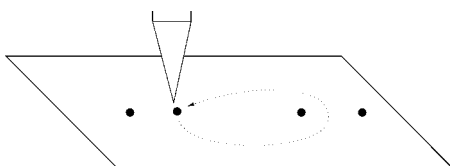


FIG. 3. Using an AFM tip to braid quasiparticles.

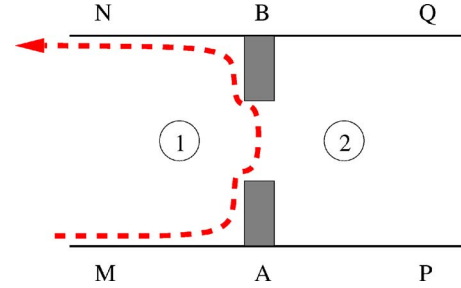


FIG. 4. (Color online) Taking a quasiparticle from the edge around one of the quasiparticles in a qubit implements a logical NOT on the qubit.

(which is presumably the magnetic length, on the order of  $100 \text{ \AA}$ ), as depicted in Fig. 3.

There is one other type of braiding process that we can do, namely taking a quasiparticle from the edge of the system around one of the quasiparticles in a qubit, as depicted in Fig. 4. Such a process is a NOT gate for this qubit.

#### B. Interferometry

The basic process by which we will determine the state of our system, i.e. read our qubits, is an interference measurement. The two states of a qubit, which differ by the absence or presence of a neutral fermion  $\psi$ , can be distinguished by taking a charge  $e/4$  quasiparticle around the pair. If the neutral fermion  $\psi$  is present, an extra  $(-1)$  occurs in the amplitude. In Ref. 19 it was shown how this minus sign could be detected by measuring the longitudinal resistance,  $\sigma_{xx}$ . It is determined by the probability for current entering the bottom edge from the left in Fig. 5 to exit along the top edge to the left. This is given, to lowest order in  $t_{MN}$  and  $t_{PQ}$ , by the interference between two processes: one in which a “test” quasiparticle tunnels from  $M$  to  $N$ ; and another in which the “test” quasiparticle instead continues along the bottom edge to  $P$ , tunnels to  $Q$ , and then moves along the top edge to  $N$ . (We subsume into  $t_{PQ}$  the phase associated with the extra distance traveled in the second process and the extra Aharonov-Bohm phase.)

$$\sigma_{xx} \propto |t_{MN}|^2 + |t_{PQ}|^2 + 2 \text{Re}(t_{MN}^* t_{PQ} \langle \psi | B | \psi \rangle). \quad (13)$$

The third term is the interference between the two possible tunneling trajectories.  $|\psi\rangle$  is the state of the qubit and the test

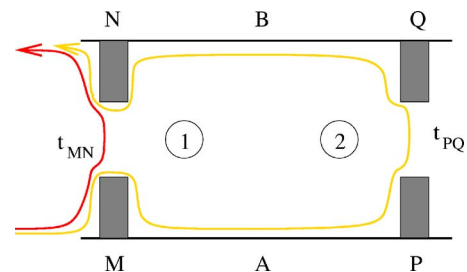


FIG. 5. (Color online) The state of a qubit can be determined from a measurement of the longitudinal conductance when inter-edge tunneling is allowed at two interfering junctions.

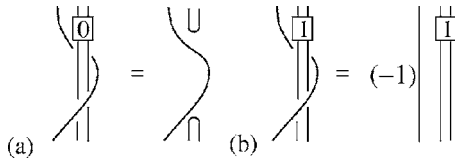


FIG. 6. The interference between the two trajectories in Fig. 5 can be obtained from the Jones polynomial (operator) evaluated on the two diagrams in this figure. In (a) the qubit is in the state  $|0\rangle$ , while in (b) it is in state  $|1\rangle$ .

quasiparticle, and  $B$  is the operator that takes the test quasiparticle around the qubit, i.e., the braiding matrix.<sup>15</sup> It can be computed by any of three equivalent ways: (1) taking  $\eta_3$  around  $\eta_1$  and  $\eta_2$  in Eq. (9); (2) using the expression in (11); or (3) by evaluating the Jones polynomial at  $q=e^{\pi i/4}$  for the link diagrams in Fig. 6 (see Appendix A for more on the meaning and an evaluation of these diagrams). Either of these methods shows that  $\langle\psi|B|\psi\rangle=\pm i$  for the two states of the qubit (the factor of  $i$  comes from the Abelian sector of the theory). Hence,

$$\sigma_{xx} \propto |t_{MN} \pm it_{PQ}|^2. \quad (14)$$

with the  $+$  sign corresponding to the state  $|0\rangle$  and the  $-$  sign corresponding to the state  $|1\rangle$ .

In the many-qubit device of Fig. 1, we would need tunnel junctions on either side of each qubit. By doing a sequence of tunneling conductance measurements, we could read each qubit in succession.

The presence or absence of a charge  $e/4$  quasiparticle on an antidot can, of course, be detected simply by measuring the charge on the antidot. However, we will have occasion to measure the topological charge contained within some complicated spacetime loops, so it will also be useful to detect charge  $e/4$  quasiparticles by interferometry. This can be done using the experimental setup of Refs. 15 and 26 as analyzed in Refs. 27 and 28. When a charge  $e/4$  quasiparticle is present on the antidot in Fig. 7, the authors of Refs. 27 and 28 showed, the two trajectories do not interfere at all because  $\langle\psi|B|\psi\rangle=0$  for Eq. (13) applied to this setup. This may be seen by evaluating the Jones polynomial at  $q=e^{\pi i/4}$  for the first link in Fig. 25, later (see Appendix A for more details).

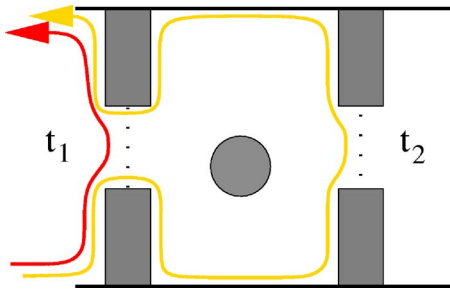


FIG. 7. (Color online) When there is a charge  $e/4$  quasiparticle at the antidot in the middle of the device, then there is no interference between the two trajectories from  $X$  to  $Y$  contributing to the longitudinal conductance.

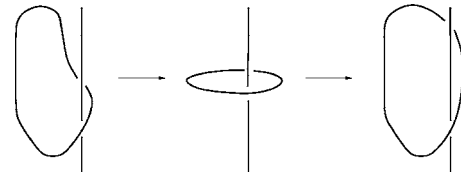


FIG. 8. A quasiparticle trajectory that winds around the antidot (straight line) can be deformed into a single time slice or stretched over a long time.

Hence,  $\sigma_{xx} \propto |t_1|^2 + |t_2|^2$ . Varying the phases of  $t_1$  and  $t_2$  will not affect the longitudinal conductivity, which is the signature of a  $\sigma$  particle.

### C. Tilted Interferometry

We now consider a generalization of the interferometry measurements of the previous subsection. Consider the diagram of Fig. 8, in which a quasiparticle-quasihole pair is created, one member of the pair winds around another quasiparticle fixed at an antidot, and then the pair is again annihilated. This picture has a special feature, namely that the quasiparticle-quasihole loop can be continuously deformed into a single time slice or, for that matter, stretched out so that it takes place over a very long time, as in the third picture in Fig. 8. Because the antidot is simply sitting there passively, the evolution in the time direction can be chosen to our advantage.

The amplitude for such a process is a measure of the total topological charge of the planar region bounded by this loop when deformed into a single time slice (as in the middle picture in Fig. 8)—in other words, it measures the topological charge on the antidot. However, we are also free to consider such processes even when they do not have an interpretation in terms of the charge in some region of a fixed time-slice plane. This type of process can occur when the spacetime topology is nontrivial. For instance, if the system is on a torus, then there is a process in which a quasiparticle-quasihole pair is created, the quasiparticle taken around the meridian of the torus until it again meets the quasihole, and they are both annihilated. The corresponding loop does not enclose any region, so the usual interpretation is not available. Such loops are an important part of the Bravyi-Kitaev construction that we describe in Sec. VI. An even more exotic possibility is depicted in Fig. 9. Suppose we have two antidots that we bring close together so that they fuse for a short period of time  $T$  before we pull them apart again. The spacetime diagram for this process is depicted in Fig. 9. Now consider a test quasiparticle that travels between the two dots. We have drawn two interfering trajectories that the test quasiparticle can take, labeled  $p$  and  $p'$  in Fig. 9. One of these trajectories,  $p$ , passes between the antidots before the merger while the other,  $p'$ , passes between the antidots after the merger. The curve  $\gamma$  captures the matrix element for the interference between these two trajectories.

Ordinarily, one thinks of the amplitude of Fig. 9 as being quite different from the middle one in Fig. 8 (for instance, in Yang-Mills theory, a Wilson loop in the time direction is a measure of the force between separated charges, and there-

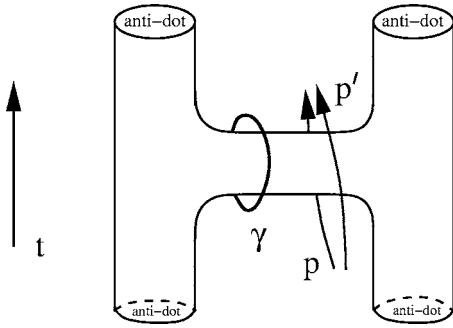


FIG. 9. Two antidots are merged for a short while and then separated again. The spacetime curve  $\gamma$  encircles the merger region. The interference between the trajectories  $p$  and  $p'$  measure the topological charge around this curve.

fore is a probe of confinement). However, in a topological phase, the curve  $\gamma$  in Fig. 9 is put on the same footing as the loop in Fig. 8 (see Appendix A for more on the relation between these diagrams and matrix elements in the Chern-Simons theory). In a topological phase, the system does not know about any preferred metric (at least at long distances and low energies), so the time direction is just as good as a spatial direction. The results of such interferometry measurements correspond to topological charges, even though there is not an interpretation as the topological charge enclosed within a spatial loop. This may be familiar to some readers in the context Laughlin states in the quantum Hall effect. At  $\nu = \frac{1}{3}$ , an interference experiment around the meridian of a torus can return as its answer  $q = 0, \frac{1}{3}, \frac{2}{3}$  (modulo 1). Of course, the meridian of the torus does not enclose a region, so these are not charges enclosed within a meridional loop. Rather, these results correspond to the different possible quasiparticle boundary conditions (monodromies) around the meridian (namely  $\psi \rightarrow e^{2\pi im/3} \psi$ ,  $m = 0, 1, 2$ ) that are the same as the phases that a quasiparticle would acquire in going around a region containing charges  $q = 0, \frac{1}{3}, \frac{2}{3}$ . Similarly, in the Pfaffian state tilted interferometry experiments will return as their result either 1,  $\sigma$ ,  $\psi$ , just as ordinary interferometry does.

Such measurements, in which quasiparticles encircle the time-dependent trajectories of quasiparticles on antidots, will be important for the protocols proposed in this paper, so it is worth spending a little time determining the limitations on such measurements, which we will call “tilted interferometry” because the curve  $\gamma$  cannot be deformed into a single time slice. (We thank Ady Stern for pointing out that tilted interferometry is analogous to the less well-known experiment proposed by Aharonov and Bohm,<sup>29</sup> in which the time dependence of  $A_0$  affects quasiparticle interference between trajectories that do not pass through regions of a finite electric (or magnetic) field.)

Unlike in the case of “ordinary” interferometry, a tilted measurement cannot, strictly speaking, be a dc measurement. In an ordinary interference experiment, the different interfering quasiparticle wave functions are plane-wave-like states, hence, even though the travel time for the two trajectories in Fig. 5 will be different, the wave functions will have a spatiotemporal overlap, so they will still be able to interfere.

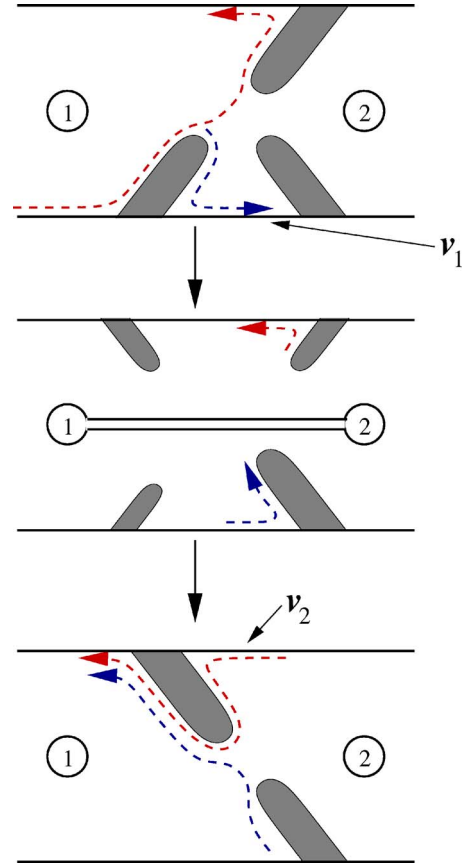


FIG. 10. (Color online) Two antidots are merged for a short while and then separated again. By putting delays into the possible quasiparticle trajectories (depicted in red and blue), we can enable them to interfere. In order to give the two antidots enough time to merge, we might wish to make the velocities  $v_1, v_2$  small.

Consider, however, the trajectories in Fig. 9. Let us suppose that the two antidots are merged from time  $t_1$  until time  $t_2$ . Then the first trajectory between the antidots must occur before  $t_1$  while the second trajectory must occur after  $t_2$ . The only way that the wave functions for the two quasiparticle trajectories can have an overlap is if there is a delay built into the first trajectory that will allow the second one to “catch up.” This can be done as shown in Fig. 10. We turn on and off some of the gates in order to direct the quasiparticles along the specified trajectories. It will also be helpful to vary the quasiparticle velocities, as also shown in the figure.

#### IV. TOPOLOGICAL PROTECTION

The main advantage of using a topological state as a platform for quantum computation is that such states have intrinsic fault tolerance.<sup>20</sup> The multi-quasihole states cannot be distinguished by local measurements, as long as the quasiholes are kept far apart. Hence, interactions with the environment, which are presumably local, cannot cause transitions between different topologically degenerate states nor can it split them in energy. Suppose that we have  $2n$  quasiparticles in our system, which is the device of Fig. 1. One might worry, for instance, that there could be a local voltage fluctuation

tuation at one of the antidots. This has a trivial effect, however: the voltage fluctuation changes the energy of all  $2^n$  states of our Hilbert space by precisely the same amount. Thus, it does not apply a phase gate, as could occur in a nontopological quantum computing scheme. The only way in which errors can occur is if a stray quasiparticle (created by the interaction with the environment) moves across the system and spontaneously performs a topological operation such as the braiding operation of Fig. 4 or the interference measurement of Fig. 5. This is closely related to the longitudinal resistance, which is the probability of an event in which a quasiparticle travels from one end of the system to another. If the spacing between antidots is large enough that quasiparticle transport at this scale is in the Ohmic regime, then the error rate and the longitudinal resistance will be controlled by the same kind of processes. (We thank Leon Balents for a discussion of this point.) Experimentally, the longitudinal resistance is observed to be in the thermally activated regime. Hence, it is limited by the density of thermally excited quasiparticles, which is exponentially small,  $\sim \exp(-\Delta/k_B T)$ , where  $\Delta$  is the quasiparticle energy gap and  $T$  is the temperature.<sup>30</sup> In Ref. 19 the resulting error rate  $\Gamma$  was estimated to be

$$\frac{\Gamma}{\Delta} \sim \frac{k_B T}{\Delta} e^{-\Delta/k_B T}. \quad (15)$$

In order to minimize the error rate, we want the temperature to be as low as possible, and we want the gap to be as large as possible, which seems to be aided by ultrahigh mobility samples. The lowest temperature reached in the experiment of Ref. 5 was  $T=5$  mK, while the measured gap was  $\Delta/k_B = 0.5$  K. This leads to an error rate of less than  $10^{-30}$ .

Of course, quasiparticles cannot be kept infinitely far apart, so there will be some splitting between multiquasihole states. This splitting can be understood as the formation of a band of propagating Majorana fermion modes, which mix the localized states. The width of this band will be proportional to the tunneling matrix element between two quasiholes, which should decay as  $w \sim e^{-R\Delta/c}$ , for some constant  $c$ , with dimensions of velocity, where  $R$  is the distance between quasiholes and  $\Delta$  is the quasiparticle gap. The condition that the quasiparticles should be kept far apart can be translated into the statement that braiding operations should be done on time scales shorter than  $1/w$ . By keeping  $R$  large compared to the inverse of the gap we can ensure that this will always be the case.

When quasiparticles are brought close together, however, there is no longer exponential protection. Suppose, for instance, that we merge two antidots into one large antidot of radius  $\rho$ . The splitting between the states  $|0\rangle$  and  $|1\rangle$  is now determined by processes in which a quasiparticle-quasihole pair is created at the edge of the antidot; they move in opposite directions around the antidot, and annihilate on the other side. Since there is no gap for the creation of quasiparticles at the edge of the antidot, there is no longer exponential suppression of such a process. Instead, it leads to a splitting  $w \sim 1/\rho$ . This means that the resulting phase error will be small if two quasiparticles are merged into a large antidot

for a short period of time, even though the protection is not as good as exponential. However, there is still topological protection against bit flip errors since these would require a neutral fermion to tunnel to or from the qubit.

A second aspect of topological protection is the exactness of braiding operations. In the case of, say, spin qubits, gates are necessarily noisy because they depend on our ability to precisely tune the duration of a  $\pi$  pulse or the strength of an applied magnetic field, which is necessarily imperfect. When gates are applied by braiding quasiparticles, however, no such tuning is necessary. The process is discrete: we either braid two quasiparticles or we do not, and if we do braid them, then the corresponding unitary transformation occurs with the same level of exactness as the vanishing of the longitudinal resistivity or the quantization of the Hall resistivity.

However, one might wonder what happens if a quasiparticle only goes  $359^\circ$  around another. If our qubits were quasiparticle pairs that we created out of the vacuum and then measured after annihilating them again in pairs at the end of the computation, then it would be clear that we would be dealing with closed braids. As long as the topological class of the closed braid traced out by the entire history of the system were preserved, it would not matter whether one quasiparticle went  $360^\circ$  around another or only part of the way around. However, we envision measuring our qubits through a quantum interference measurement of the topological charge around some closed curves. Therefore, we will consider this issue in a little more detail. If one quasiparticle were to go  $360^\circ$  around another then the initial and final states of the system lie in the same Hilbert space and the action of the braiding operation is just its unitary representative on this Hilbert space. However, if a particle only goes  $359^\circ$  around another, then the initial and final states of the system do not lie in the same Hilbert space. Of course, the initial and final Hilbert spaces are unitarily equivalent, but the problem is that a unitary transformation between them could be trivial or it could undo the braiding operation. So what happens? The answer is that it depends on how the system is now measured. If the state of the system is measured by interference, then the result will depend on what path the interfering test quasiparticle takes (incidentally, this is always true since we can undo the effect of a braid by choosing a convoluted interfering path). If a particle goes  $359^\circ$  around another, then almost all paths will give a result that is the same as if it had gone  $360^\circ$ . In other words, it is not necessary to have very precise control of quasiparticle positions. Of course, if a quasiparticle were to only go  $270^\circ$  around another, then we would have to exercise more care in choosing a trajectory for a test quasiparticle. However, even as drastic a deviation as this is not that serious a problem. The same caution holds if, instead of measuring the system, we wanted to act on it with yet another braiding operation. An example of such a situation is given in Fig. 11. The same logic also holds for the uncontrolled motion of a stray quasiparticle; whether or not it has moved far enough to cause an error will depend on how the qubit is subsequently measured.

A potential second source of error is braiding operations that are performed too quickly. The time scale  $t_{\text{op}}$  over which

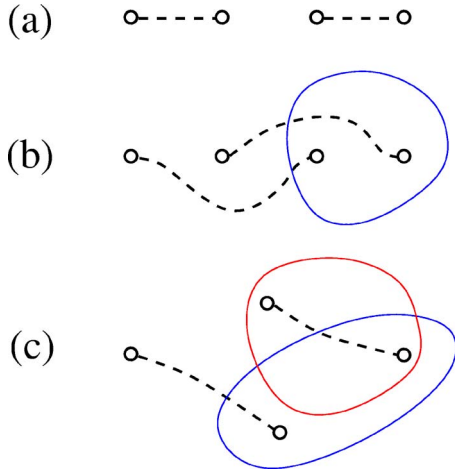


FIG. 11. (Color online) In (a), we have two pairs of quasiparticles. The dashed lines connect quasiparticles that fuse to form the (topologically) trivial particle. In (b), the second and third quasiparticles are exchanged. A measurement of the topological charge around the blue curve or an operation that takes another quasiparticle around this curve will give a nontrivial result as a result of this exchange. The same result is clearly obtained even if the final position of the quasiparticles is slightly different from those shown. If the exchange is incomplete, as in (c), then a measurement around the blue curve will give a non-trivial result but a measurement around the red curve will give a trivial result. As long as we are careful to measure the system with the blue curves in (b) and (c), we will find the correct result.

a braiding operation is done must be slow compared to the gap,  $t_{\text{op}} \gg 1/\Delta$ . If this inequality is violated, a pair of quasiparticles might be created. These quasiparticles might then execute a nontrivial braid before annihilating each other (the Coulomb blockade presumably prevents them from annihilating the quasiparticles on the antidots), thereby applying  $g \cdot g'$ , for some  $g'$ , rather than our intended gate  $g$ . The amplitudes for various  $g'$  depend on the ability of quasiparticles to move around the system (semiclassically, a random walk). To avoid such errors, we must make sure that such quasiparticles are not created in the first place by performing all braiding operations slowly,  $t_{\text{op}} \gg 1/\Delta$ . Again, it is advantageous to make the gap  $\Delta$  as large as possible.

While the braiding operations and interference measurements described in this paper are similar in the sense that they both involve topological operations, they are actually quite different in an important respect. The braiding operations by which we envision manipulating our qubits are *unitary operations*. They involve moving quasiparticles around our system over time scales that must be long compared to the inverse of the gap and small compared to the inverse of the error rate:

$$\frac{1}{\Delta} \ll t_{\text{op}} \ll T e^{\Delta/T}. \quad (16)$$

As long as this order of time scales is respected and the quasiparticles are kept far apart (compared to the magnetic length, which is the only length scale in the problem), then

the system is topologically protected: the quantum state of the system evolves precisely as we specify.

On the other hand, our interference measurements are dissipative dc measurements (since they require nonzero  $\sigma_{xx}$ ). As far as the multiqubit Hilbert space is concerned, these are not unitary operations but, rather, projection onto specified states. It is worthwhile thinking a little more about how this “wave function collapse” occurs because these measurements are potentially noisy. For instance, if a current-carrying edge quasiparticle were to scatter inelastically, then the interference between its two possible trajectories will be spoiled. If this inelastic scattering rate becomes too large, then we will be unable to read the state of our quasiparticles through an interference measurement because we will not be able to resolve two different values of the longitudinal conductivity. We would like to know when this will occur. Also, when this occurs, there is an interesting quantum measurement theory problem: does the qubit wave function still “collapse” even when the inelastic scattering rate for the test particles is too high to allow us to distinguish the two states of the qubit?

To answer these questions, we begin by considering Fig. 5. When a single test quasiparticle tunnels between the two edges (without scattering inelastically), its wave function becomes entangled with the state of the qubit: it is in one state, which we will call  $|a\rangle$  when the qubit is in the state  $|0\rangle$  and it is in a different state,  $|b\rangle$ , when the qubit is in the state  $|1\rangle$ . If the initial state of the system were  $\alpha|0\rangle + \beta|1\rangle$ , then it is now

$$\alpha|0\rangle|a\rangle + \beta|1\rangle|b\rangle. \quad (17)$$

If  $|a\rangle$  and  $|b\rangle$  were the same, then there would be no entanglement with the test quasiparticle at all and the coherent superposition of  $|0\rangle$  and  $|1\rangle$  is maintained. However, if  $|a\rangle$  and  $|b\rangle$  were orthogonal, then the entanglement between the qubit and the test quasiparticle would completely spoil the coherent superposition of  $|0\rangle$  and  $|1\rangle$  (unless they can be disentangled later), i.e., the qubit wave function is ‘collapsed’.

For small tunneling amplitudes  $t_{MN}$  and  $t_{PQ}$ , both  $|a\rangle$  and  $|b\rangle$  are concentrated on the bottom edge in Fig. 5, and there is very little difference between these two states of the test quasiparticle. We can write

$$\langle b|a\rangle = 1 - \delta, \quad (18)$$

with  $\delta$  small. Hence, a single test quasiparticle does not do an effective job of “collapsing” the qubit wave function. In order to be an effective measurement, we would like the qubit to be in the state  $|0\rangle$  with probability 1 when the test quasiparticle is in the state  $|a\rangle$ . When (18) holds, the qubit is instead in the state  $\alpha|0\rangle + \beta(1 - \delta)|1\rangle$  when test quasiparticle is in the state  $|a\rangle$ .

However, if  $N$  test quasiparticles tunnel, then they all become entangled with the qubit. The combined state of the qubit and test quasiparticles is

$$\alpha|0\rangle|a,a, \dots, a\rangle + \beta|1\rangle|b,b, \dots, b\rangle. \quad (19)$$

Notice that we now have

$$\langle b, b, \dots, b | a, a, \dots, a \rangle = (1 - \delta)^N. \quad (20)$$

For  $N$  sufficiently large, these states are nearly orthogonal. Hence, the two states of the qubit cannot be coherently superposed unless the qubit is disentangled from the test quasiparticles. This cannot happen once the test quasiparticles leave the system at the current lead and thermalize there, which is an irreversible process. Thus, we conclude that the qubit wave function “collapses:” when the test quasiparticles are all in the state  $|a\rangle$ , the qubit is in the state  $|0\rangle$  with probability  $1 - (1 - \delta)^{2N}$ , which is  $\approx 1$  for  $N$  large.

Now, consider the effect of inelastic scattering on the test quasiparticles. Those test quasiparticles which are inelastically scattered, do not become entangled with the qubit. As far as measuring the qubit is concerned, we can forget about them. However, as long as there is a large number  $N$  of quasiparticles that coherently encircle the qubit without inelastically scattering, the qubit wave function will collapse, according to the previous logic. In principle, we can always ensure that this happens simply by waiting long enough, but once the inelastic scattering rate becomes of order  $\Gamma_{cr} \sim v/L$  where  $L$  is the device size and  $v$  the edge velocity, we would have to wait an exponentially long time.

The criterion for actually being able to read the value of the qubit is a little different, however. It depends on the resolution of our ohmmeter. When the inelastic scattering rate is too high, we will not be able to resolve that there are actually two different values of the longitudinal conductivity. However, depending on how accurately we can measure the longitudinal conductivity, this could occur before the bound  $\Gamma_{cr}$  is reached. Thus, it is possible that the qubit wave function might “collapse” by a measurement, even though we would not be able to read the result.

We should conclude this section with a comment directed to our topologically inclined readers (perhaps 100% of those who have come so far). Many critical details of the interferometer, such as the inelastic scattering length, travel times, quasiparticle “delays,” etc., are not topological in nature. How is this to be reconciled with the fact that in a topological theory all information on the change of state should be encoded by the 2+1-dimensional spacetime history of the medium? The answer is that the topology of various tunneling trajectories gives us operators  $h_1, h_2, \dots$ , evolving the system from initial to final states. However, experimental details determine other (dissipative) terms in the evolution equation of the density matrix of the system. In the limit that these other terms are small, a pure quantum state will remain pure and different 2+1-dimensional space-time histories will contribute coherently to the evolution of this quantum state. When they are large, a pure quantum state will evolve into a mixed one and the 2+1-dimensional space-time histories will effectively combine to form a superoperator for this mixed state density matrix.

## V. UNIVERSAL GATE SET USING SOME TOPOLOGICALLY UNPROTECTED GATES

For all of its remarkable properties, the Pfaffian state suffers from one serious drawback: the transformations gener-



FIG. 12. By bringing together quasiparticles 1 and 2, which form a qubit, we can apply the gate  $g_1$ . This operation is unprotected and requires control of the distance between the quasiparticles and the length of time that they are brought together. However, the required precision might not be very stringent as a result of the availability of topologically protected operations such as  $g_3$ .

ated by braiding operations are not sufficient to implement all possible unitary transformations.<sup>22,26</sup> Hence, these operations do not permit universal quantum computation. However, we do not need to supplement braiding with much in order to obtain a universal gate set. In this section, we explain a “quick and dirty” way of doing this.

First, consider single-qubit operations. If we bring the two quasiparticles that comprise a qubit close together, as shown in Fig. 12, then their splitting will become appreciable. This splitting has the form  $\Delta E(r) \sim e^{-r\Delta/c}$ , where  $r$  is the distance between the quasiparticles and  $c$  is some constant with dimensions of velocity. If we wait a time  $T_p$  before pulling the quasiparticles apart again, then we will apply the phase gate:

$$U_P = \begin{pmatrix} 1 & 0 \\ 0 & e^{i\Delta E(r)T_p} \end{pmatrix}. \quad (21)$$

A particularly convenient choice is  $\Delta E(r)T_p = \pi/4$ , which would allow us to apply the same transformation as the gate  $g_1$  described in the next section.

Let us further assume that we can actually perform this operation on any pair of quasiparticles, not just two quasiparticles from the same qubit. Note that in order to do this we only need precise control over the distance between one pair of antidots since we can use  $g_3$  to move any desired pair of quasiparticles to these preferred antidots (e.g., using the bucket brigade of auxiliary antidots to move quasiparticles). If we bring together in precisely the same manner two quasiparticles from different qubits, then we will couple the two qubits. In terms of the Majorana modes of (11), this gate is  $\exp[(\pi/8)\gamma_i\gamma_j]$ . [In the special case that  $i$  and  $j$  come from the same quasiparticle, this is the same as (21) up to an overall phase.]

The other gate that we need for a universal quantum computation is the nondestructive measurement of the total topological charge of any pair of qubits. This can be done by using  $g_3$  to move one qubit so that it is next to the other. Then, the interference measurement depicted in Fig. 13 can determine the sum of the topological charges of the two neighboring qubits. This is a measurement of  $\gamma_1\gamma_2\gamma_3\gamma_4$ . According to Ref. 31, this measurement is equivalent to the application of the gate  $\exp[(\pi/4)\gamma_1\gamma_2\gamma_3\gamma_4]$  as long as we have the ability to (a) create ancilla in the state  $|0\rangle$  and (b)

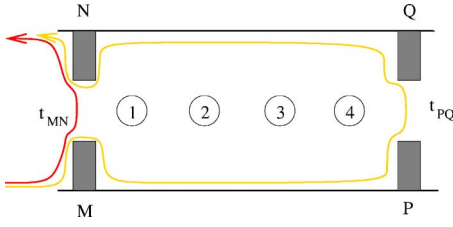


FIG. 13. (Color online) A nondemolition measurement of the total topological charge of two neighboring qubits (comprised of 1, 2 and 3, 4) can be done with the interference measurement shown here. Together with  $g_3$  and the operation  $U_P$  shown in Fig. 12, this forms a universal gate set.

apply  $\exp[(\pi/4)\gamma_i\gamma_j]$ , which is simply the exchange of quasiparticles  $i$  and  $j$ .

An obvious problem is that we have now given up some of the protection that we have worked so hard to obtain. Even if we could calculate  $\Delta E(r)$  with high precision, there would always be some chance of a mistake in the length of time  $T_p$  that the quasiparticles are close together. Thus, we would be in a situation in which some gates are exact—those resulting from braiding operations—while others are unprotected. The threshold error rate for the unprotected operations can be much less stringent (as high as 10%), as shown by Bravyi and Kitaev<sup>32</sup> for a specific set of perfect gates together with the noisy creation of a one-qubit ancilla in a specified state (a “magic state”). It is still an open problem what the threshold is for the set of protected gates and the one unprotected gate described previously.

## VI. BRAVYI-KITAEV CONSTRUCTION

In Ref. 22, Bravyi and Kitaev constructed a universal set of gates for a system in the topological phase described by the  $SU(2)_2$  Chern-Simons theory, which is the effective field theory<sup>15,16</sup> likely to describe the  $\nu = \frac{5}{2}$  quantum Hall state, apart from an Abelian factor, which is unimportant here. For reference, their gates  $\{g_1, g_2, g_3\}$  are

$$g_1 = \begin{pmatrix} 1 & 0 \\ 0 & e^{\pi i/4} \end{pmatrix}, \quad g_2 = \begin{pmatrix} 1 & 0 & 0 & 0 \\ 0 & 1 & 0 & 0 \\ 0 & 0 & 1 & 0 \\ 0 & 0 & 0 & -1 \end{pmatrix},$$

$$g_3 = \frac{1}{\sqrt{2}} \begin{pmatrix} 1 & 0 & 0 & -i \\ 0 & 1 & -i & 0 \\ 0 & -i & 1 & 0 \\ -i & 0 & 0 & 1 \end{pmatrix}. \quad (22)$$

$g_1$  is a phase gate on a single qubit.  $g_2$  and  $g_3$  are two-qubit gates.  $g_2$  is a controlled phase gate: if both qubits are in state  $|1\rangle$ , the state acquires a  $(-1)$ . Otherwise, it is unchanged. Alternatively, if we change the basis of the second qubit to  $(|0\rangle \pm |1\rangle)/\sqrt{2}$ , then  $g_2$  is simply a CNOT gate.  $g_3$  is a two-qubit gate, which, together with  $g_1, g_2$ , form a universal gate set. This particular gate is chosen because it can be imple-

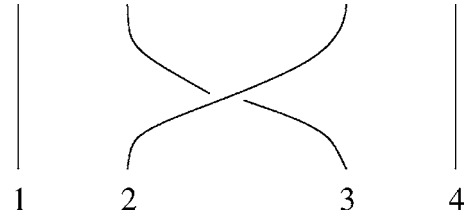


FIG. 14. Quasiparticles 1 and 2 form a qubit; 3 and 4 form a second qubit. Exchanging 2 and 3 applies the gate  $g_3$ .

mented with the simple quasiparticle braiding process depicted in Fig. 14.

The controlled phase gate  $g_2$  is more complicated. Suppose we have two qubits composed of two pairs of quasiparticles (1, 2) and (3, 4). We would like to multiply the state of the system by  $(-1)$  only when qubits (1, 2) and (3, 4) are *both* in state  $|1\rangle$ . The problem is that if qubit (3, 4) is in state  $|1\rangle$  and we take it around quasiparticle 1, then a factor of  $(-1)$  results, regardless of whether (1, 2) is in the state  $|0\rangle$  or  $|1\rangle$ . The trick of Bravyi and Kitaev<sup>22</sup> is to split qubit (1, 2) in such a way as to produce a charge  $e/4$  quasiparticle only when (1, 2) is in the state  $|1\rangle$ . If this occurs, then we can take (3, 4) around this quasiparticle, and a  $(-1)$  will occur if (3, 4) is also in the state  $|1\rangle$ .

In order to do this, we perform the following steps that we will describe here without regard to their feasibility (which will be taken up in the next section). Suppose that quasiparticles 1 and 2 are at antidots, which should be understood as punctures in the quantum Hall fluid. The state of the (1, 2) qubit is equal to the topological charge around the loop  $B_0$  in the top diagram in Fig. 15. We will denote this topological charge by  $W(B_0)$ . We create an overpass that connects these two punctures, as depicted in the middle part of Fig. 15. We check with an interferometry measurement that the boundary of the antidots-plus-overpass, labeled  $B_1$  in Fig. 15, has trivial topological charge,  $W(B_1)=1$ . If it does not, we break the overpass and rebuild it again until we find  $W(B_1)=1$ . We do not need to repeat this very often since the probability for  $W(B_1)=1$  is  $1/2$  and the probability for  $W(B_1)=\psi$  is also  $1/2$  [since the isospin 0 and 1 quasiparticles have the same quantum dimension—i.e., the same zero-temperature entropy per particle—in  $SU(2)_2$  Chern-Simons theory]. Each time we break the overpass, we return the qubit to its original state. This follows from the general principle (see Appendix B) that adding quantum media is reversible simply by deleting what was added (whereas deleting quantum media is generally irreversible).

Once we know that  $W(B_1)=1$ , it follows for reasons that we discuss below that if (1, 2) is in state  $|1\rangle$  [i.e., if  $W(B_0)=\psi$ ], then  $W(C)=\sigma$  in Fig. 15. If this is the case, then taking (3, 4) around the loop  $C$  multiplies the state by  $(-1)$  if (3, 4) is in state  $|1\rangle$  and leaves it unchanged if it is in state  $|0\rangle$ . On the other hand, if (1, 2) is in state  $|0\rangle$ , then  $W(C)=(1-\psi)/\sqrt{2}$  in Fig. 15, and taking (3, 4) around  $C$  does not change the state. Therefore, this sequence of operations applies the gate  $g_2$  of (22).

The Chern-Simons theory calculations that lead to this result are facilitated by the observation that the topology of

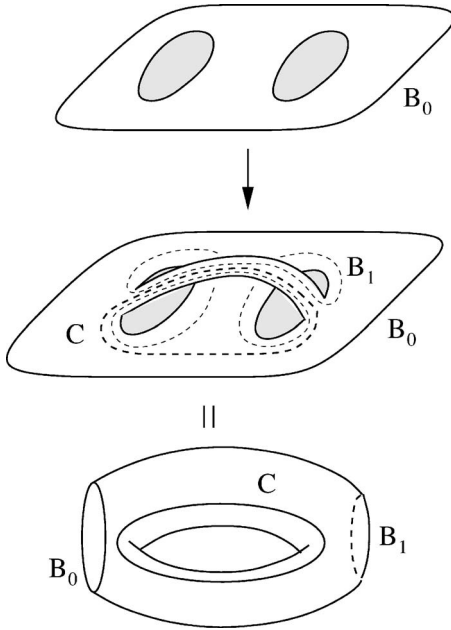


FIG. 15. By adding an overpass, we connect two antidots. The dashed curve labeled  $B_1$  is the combined boundary of the antidots-plus-overpass. In the implementation of both  $g_1$  and  $g_2$ , we need to check that  $W(B_1)=1$ . In the case of  $g_2$ , the controlled qubit must be taken around  $C$  in order to implement a controlled phase gate on it. To enact  $g_1$ , a double Dehn twist must be performed in  $C$ . The two antidots joined by an overpass in the middle of the figure are topologically equivalent to a torus with two punctures corresponding to  $B_0$  and  $B_1$  as shown at the bottom. The meridian of the torus is  $C$ .

two antidots joined by an overpass is a torus with two punctures, corresponding to  $B_0$  and  $B_1$ , as depicted in the bottom diagram of Fig. 15. The curve  $C$  is the meridian of the torus. Once we have made sure that  $W(B_1)=1$ , we know that we can fill in this puncture without changing anything; in other words, the system is equivalent to a torus with one puncture,  $B_0$ . Observe that  $W(B_0)$  is the state of the qubit: it is either 1 or  $\psi$ . We would now like to determine  $W(C)$ . This can be obtained from the  $S$  matrix of the theory, which relates the topological charge around the meridian,  $W(M)$ , to the topological charge around the longitude,  $W(L)$ . If  $W(B_0)$  is 1, the  $S$  matrix is

$$S_{ij}^1 = \begin{pmatrix} \frac{1}{2} & \frac{1}{\sqrt{2}} & \frac{1}{2} \\ \frac{1}{\sqrt{2}} & 0 & -\frac{1}{\sqrt{2}} \\ \frac{1}{2} & -\frac{1}{\sqrt{2}} & \frac{1}{2} \end{pmatrix}, \quad i, j = 1, \sigma, \psi. \quad (23)$$

However,  $W(L)$  is simply the topological charge on each of the antidots, which is  $\sigma$  [i.e.,  $(0, 1, 0)$  in the matrix notation of (23)]. Hence, the  $S$ -matrix tells us that  $W(C)$  is the linear combination  $(1-\psi)/\sqrt{2}$ . On the other hand, if  $W(B_0)=\psi$ , then the vanishing of all  $S$  matrix elements  $S_{ij}^\psi$  other than  $S_{\sigma\sigma}^\psi = e^{-i\pi/4}$  tells us that  $W(C)=\sigma$ .

We now turn to  $g_1$ . The first step in the implementation of gate  $g_1$  in (22) is the same as previous: we take the two antidots associated with the qubit under consideration and join them with an overpass as in Fig. 15. Again, we check that  $W(B_1)=1$ . Now, however, we act on this qubit by performing a double Dehn twist on the curve  $C$ . This means that we cut along the curve  $C$ , thereby forming two boundaries. We rotate one of them by  $4\pi$  relative to the other (i.e., perform two twists) and then glue them back together. Finally, we remove the band, thereby returning the system to a state of two  $\sigma$  quasiparticles, one on each of the two antidots.

A Dehn twist on  $C$  has an equivalent effect as a  $2\pi$  rotation of the topological charge associated with  $C$ . Since the conformal spins of 1,  $\sigma$  and  $\psi$  are, respectively, 0,  $\frac{1}{16}$ , and  $\frac{1}{2}$ , the effect of performing two successive Dehn twists is simply the identity  $1^2=(-1)^2$  if  $W(C)$  is, respectively, 1 or  $\psi$  and it is  $(e^{2\pi i/16})^2=e^{\pi i/4}$  if the topological charge is  $\sigma$ . Since  $W(C)$  is perfectly correlated with the value of the qubit, the effect of this sequence of operations is the gate  $g_1$  in (22). Note that a single Dehn twist would necessarily change the charge of the two antidots by transferring charge  $e/4$  from one to the other.

## VII. FROM NONPLANAR TOPOLOGY TO TIME-DEPENDENT PLANAR TOPOLOGY

The operations described in the previous section may never be practical in a real quantum Hall device. Overpasses with high mobility are implausible, let alone gating them in and out at will. Dehn twists seem an even more remote possibility. Fortunately, there are some features of Chern-Simons theory, which is the effective field theory of our system, which can be exploited to mimic these types of operations without leaving the plane or attempting to perform surgery on our quantum Hall fluid. In this section, we will explain these features of Chern-Simons theory and how they can be used to apply the gates  $g_1$  and  $g_2$ . Once this problem in topological quantum field theory (TQFT) has been solved, we turn in the next section to the new set of problems that arises when we try to realize this construction in a quantum Hall device. For the reader who is uninterested in the TQFT details and wishes to skip ahead to the next section, we summarize the results of this section: (1) an operation equivalent to the addition and removal of an overpass between two antidots can be performed by connecting the two antidots as long as a curve surrounding the connection (which might be tilted) has a trivial topological charge; (2) a measurement of the topological charge around a curve  $\gamma$  (with a particular framing) is equivalent to a ‘‘Dehn filling’’ on this curve (which, in turn, is related to a Dehn twist, as explained below) modulo a few caveats described in this section. With these two observations in hand, we can replace ‘‘impossible’’ operations with operations that are merely very difficult. In Sec. VIII, we give concrete illustrations of how this can be done with the device architecture described in this paper.

One particularly fortuitous feature of topological field theories, for our purposes, is the fact that when the topological charge around a hole is trivial, then the part of the system

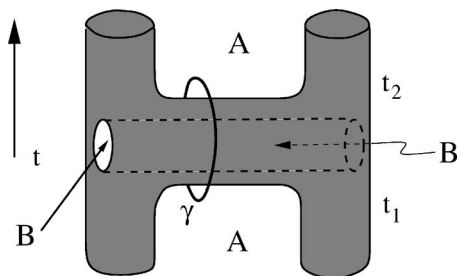


FIG. 16. A nonplanar overpass configuration can be mimicked by breaking the region  $A$  and adding  $B$ . This is done by merging the two antidots between times  $t_1$  and  $t_2$ . During this merger interval, we allow the quantum Hall fluid to fill the region  $B$ . This faux pass splits the merged antidot in the perpendicular direction. These changes are then undone to return the system to its initial configuration. In order to verify that removing  $A$  was harmless, we have to perform a tilted interferometry measurement to check that the topological charge around  $\gamma$  is trivial. See Fig. 20, later, for a time slicing of this process.

outside the hole is impervious to whether the hole is filled in or not. For example, if the topological charge around  $\gamma$  in Fig. 9 is trivial, then this spacetime history is equivalent, as far as a topological field theory is concerned, with a spacetime history in which there is no merger whatsoever between the two antidots. This suggests a way in which we can effectively have overpasses by taking advantage of the time direction so that “over” is realized as “at a different time,” as shown in Fig. 16. Suppose we want a band of material  $B$  to form an overpass over another band  $A$ . We instead break  $A$  at time  $t_1$ , allow  $B$  to pass, use  $B$  for whatever purpose, break  $B$ , and then reconstitute  $A$  at time  $t_2$ . If we could measure the topological charge around the resulting timelike hole  $t_1 < t < t_2$  in  $A$  and if we found that it was trivial, it would be, as far as Chern-Simons theory were concerned, as if  $A$  were never broken. The faux overpass—or, simply, faux pass— $B$  is then just as good as an overpass.

Note that this figure can be continuously deformed to our convenience. From a topological point of view, Fig. 16 is equivalent to Fig. 17. However, their realizations are quite different, and they have different practical advantages and disadvantages. The tilted measurement of  $\gamma$  in Fig. 16 is untilted in Fig. 17. However, Fig. 17 has a moving antidot and island (whose velocity is the slope of the faux pass in Fig. 17).

A second “impossible” operation which we need to perform is a Dehn twist on a closed curve  $C$ . In order to make it possible, we use the following two facts. (i) It is a fundamental identity of the “Kirby calculus” that  $(-1)$ -framed “Dehn surgery” on a simple linking circle imparts a  $(+1)$  Dehn twist and, of course, a double Dehn twist arises if two such surgeries are performed. By “frame,” we mean that the curve  $C$  is thickened into a ribbon so that a self-linking number can be well defined: it is the linking number of the two curves formed by the edges of the ribbon (one edge of the ribbon is  $C$ , the other edge is traced out by the tip of the frame vector). Some examples of framed curves are shown in Fig. 18. We would like  $C$  to be framed so that this self-linking number is  $(-1)$ . The meaning of “Dehn surgery” is that a tubular neighborhood

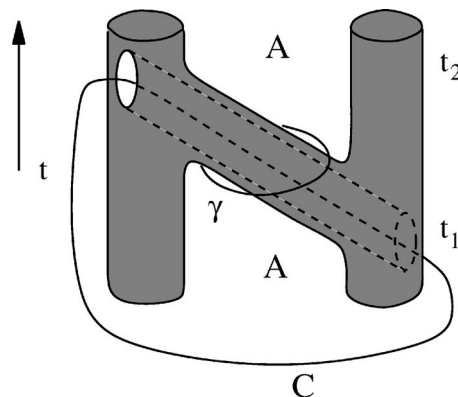


FIG. 17. Topologically, the process depicted here is equivalent to that depicted in Fig. 16. However, as a result of the tilt of the faux pass, the triviality of the charge around the hole in  $A$  can be measured with an untilted measurement. Consequently, the curve  $\gamma$  can now be deformed into a single time slice. The curve labelled  $C$  in this figure is equivalent to the curve  $C$  that goes over the overpass in Fig. 15. This is the curve on which we wish to perform a Dehn twist. Measuring the topological charge around this curve allows us to effect the same transformation on the quantum state of the system without any surgery. See Fig. 24, later, for a time slicing of this process.

neighborhood (in spacetime) of the loop  $C$  is deleted and then glued back so that the meridian disk is glued to the circle defined by the tip of the frame vector. Obviously, physical limitations prevent us from doing this in a quantum Hall device, but we can instead (ii) measure the particle content of a loop  $\zeta$  in the interior of a  $2+1$ -dimensional space-time. If the result is 1, we have (up to an overall normalization factor, corresponding to capping a 2-sphere) accomplished Dehn surgery on  $C$  as far as the Chern-Simons theory is concerned. This Dehn surgery on a spacetime history has the result of making it into a history that interpolates between an initial state before a Dehn twist has been performed on the faux pass and a final state in which the faux pass has been Dehn twisted.

We would like to explain the relation between Dehn twist, Dehn surgery, and Dehn filling. The Dehn twist is a method for constructing a diffeomorphism of a surface: given a closed loop  $l$  on a surface, cut the surface along  $l$ , twist one side by  $2\pi$  and reglue. This is either a  $+$  or  $-$  Dehn twist

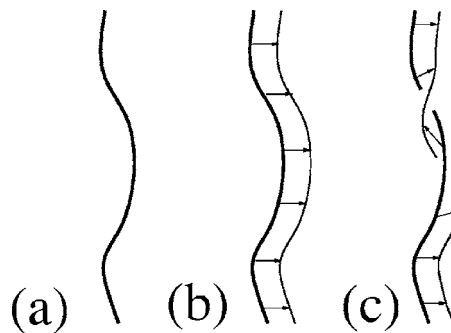


FIG. 18. The curve in (a) can be framed, for example, as shown in (b) and (c). The self-linking number in (c) is greater by  $+1$  than in (b).

(depending on sign conventions). Our interest in Dehn twist is that it provides a way to transform a 3-manifold  $M$  by cutting it open along a surface and then regluing using a Dehn twist. To discuss this procedure, we will simplify matters by concentrating on an annular neighborhood  $A$  of  $l$ . (The framing of  $l$  defines an annulus  $A$ , as may be seen in Figs. 18(b) and 18(c). We split the 3-manifold  $M$  along  $A$ , thereby opening a toridal cavity within  $M$ . The boundary of this cavity is a torus  $B$ , which is just two copies of  $A$ , joined along their boundaries. This new manifold with the cavity is essentially  $M \setminus \text{neigh}(l)$ ,  $M$  minus a neighborhood of  $l$ . The term “Dehn filling” refers to gluing a solid torus back into the cavity; the double process of first making the cavity and then refilling it is called “Dehn surgery.” The possible outcomes of Dehn surgery are parametrized by the slope of that curve on the cavity boundary  $B$  that is matched to the disk factor  $D^2$  of the reglued solid torus  $D^2 \times S^1$ . Notice that Dehn twist, from one copy of  $A$  to the other, carries a radial arc in one copy to a twisted arc in the other so that the two mate together to become a diagonal—either  $(1,1)$  or  $(1,-1)$  in the natural  $B$  coordinates (the first component counts the winding number around the “meridian” or the shortest direction and the second coordinate counts the winding number around the “longitude” defined by either component of the boundary of  $A$  within  $B$ ) depending on whether the Dehn twist is  $+$  or  $-$ , respectively. Conversely, the instruction to do “ $-1$  Dehn surgery on  $l$ ” can be expressed as follows: (1) open the cavity around  $l$  (a normal framing on  $l$  is required at this point to pick out the surface  $A$ ); (2) change the correspondence between the two copies of  $A$  by  $a+1$  Dehn twist; (3) with respect to these new coordinates, Dehn fill the solid torus by gluing the disk to the meridian of the cavity. [Steps (2) and (3) together constitute  $-1$  Dehn filling since they tell us to match the  $(1,-1)$  curve on the cavity boundary  $B$ , which is taken to the meridian by step 2, to the disk within the reglued solid torus.] Thus cutting and regluing by a  $+/-$  Dehn twist is identical to doing  $+/-$  Dehn surgery. The latter is simply a more three dimensional language for the former. Measuring the trivial charge along a curve  $C$  is, from the point of view of Chern-Simons theory, equivalent to supplying a disk (containing no quasiparticles) for the curve  $C$  to bound, or an entire solid torus (with no Wilson loop at its core) for  $B$  to bound. Thus, we propose to accomplish through measurement a topological operation, namely Dehn twist, which otherwise would have no reasonable experimental realization.

An important detail to be considered is that measurement might result in a nontrivial charge. This means, in fact, that the reglued solid torus does carry a Wilson loop of precisely that charge. This Wilson loop is depicted in Fig. 19 as a loop  $\beta$  in the exterior solid torus, as shown. These states with Wilson loops correspond to the other two ground states on the torus (up to an additional factor of 2 degeneracy coming from the Abelian part of the theory). These are the states obtained by performing the Chern-Simons functional integral over a solid torus with a Wilson loop carrying topological charge ( $\sigma$  or  $\psi$ , resp.), but expressed in the meridinal basis.

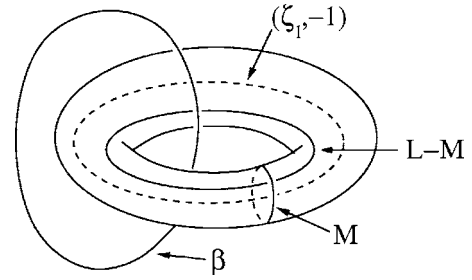


FIG. 19. If we measure the topological charge around  $(\zeta_1, -1)$  and it is not 1, then we have performed a Dehn filling on  $(\zeta_1, -1)$  and left behind a Wilson loop  $\beta$ , carrying this topological charge, inside the solid torus. The state of the system is given by the functional integral in Eq. (24) for this manifold. The 3-D mapping cylinder of a Dehn twist can be described as follows: delete a solid torus, then replace it with a twisted Dehn filling. For convenience, we have drawn the torus in a nonstandard way so that  $L-M$  appears simple.

$$\Psi[a] = \int_{A|_{T^2=a}} DA W[A, \beta] e^{\int_M \mathcal{L}_{CS}[A]}, \quad (24)$$

where  $\mathcal{L}_{CS}[A]$  is the Chern-Simons Lagrangian and  $M = D^2 \times S^1$  is the solid torus.  $W[A, \beta]$  is the Wilson loop (i.e., the trace of the holonomy of the gauge field  $A$ ),  $W[A, \beta] = \text{Tr}[\mathcal{P} \exp(\oint_{\beta} A)]$ , with the trace taken in the fundamental or the adjoint representation (for, respectively,  $\sigma$  or  $\psi$ ), and the functional integral is over  $SU(2)$  gauge fields  $A$  such that  $A = a$  on  $T^2$ , the boundary of the solid torus. Since the Wilson loop must be around the meridian,  $\beta$  is depicted as “outside” the torus in Fig. 19.

In order to perform a double Dehn twist on  $C$ , we need to measure the topological charge around two framed curves that run parallel to  $C$ . We will call these curves  $(\zeta_1, -1)$  and  $(\zeta_2, -1)$ ; the  $-1$  denotes the framing. Note that  $C$  is equivalent to untwisted copies of the  $\zeta$ 's, which can be denoted  $(\zeta_1, 0)$  and  $(\zeta_2, 0)$ . In order to measure the topological charge around  $(\zeta_1, -1)$  and  $(\zeta_2, -1)$ , our measurement quasiparticles will have to go along a curve with an extra twist; a way of realizing this is shown later in Fig. 23. If a measurement finds  $W(\zeta_1) = 1$ , then we have performed the desired Dehn twist. Finding  $W(\zeta_1) = \psi$  is not the end of the world because the extra Wilson loop that results just gives some extra minus signs. However, we want to avoid  $W(\zeta_1) = \sigma$ . One way to do this is to take a charge  $\sigma$  around the loop  $(\zeta_1, 0)$ . Then let  $(\zeta_1, -1)$  run parallel to the charge, encircling it to yield the framing  $(-1)$ . Later, in Fig. 23, we have depicted a time slicing of such a framed curve: the measurement quasiparticle must wind around the quasiparticle, that is following the loop  $(\zeta_1, 0)$ .

We can now use a similar argument to that used after (23) to show that  $W(\zeta_1) = (1 - \psi) / \sqrt{2}$ : since  $(\zeta_1, -1) = L - M$  (i.e., longitude-meridian), we claim that  $W(\zeta_1)$  is given by  $ST^{-1}|\sigma\rangle$ , where  $n$ ,

$$S = \begin{pmatrix} 1/2 & \sqrt{2}/2 & 1/2 \\ \sqrt{2}/2 & 0 & -\sqrt{2}/2 \\ 1/2 & -\sqrt{2}/2 & 1/2 \end{pmatrix} \text{ and } T = \begin{pmatrix} 1 & 0 & 0 \\ 0 & e^{i\pi/8} & 0 \\ 0 & 0 & -1 \end{pmatrix},$$

in the  $\{1, \sigma, \psi\}$  basis. We check that  $ST^{-1}|\sigma\rangle = e^{-i\pi/8}(|1\rangle - |\psi\rangle)/\sqrt{2}$ . Hence, a measurement of  $W(\zeta_1)$  can only give 1 or  $\psi$  (with equal probabilities). By doing this with another charge, parallel to  $\zeta_2$  and encircled by it, we can force a measurement of  $W(\zeta_2)$  to be 1 or  $\psi$ , again with equal probabilities, and completely independent of the result of the  $W(\zeta_1)$  measurement.

To see that  $ST^{-1}$  gives the correct transformation, note that we wish to transform from the longitudinal basis  $L$  to the framing  $= k$  basis,  $L + kM = \text{longitude} + k(\text{meridian})$ . To define a basis  $V(T^2) = \sum_{\text{particle types}, a} V_{a\bar{a}}(S^1 \times I)$ , we need to select a circle, the ‘‘cuff,’’ to cut the torus along a dual circle, the ‘‘seam,’’ to trivialize the resulting annulus as  $S^1 \times I$ . The transformation is then done in the following two steps:<sup>33</sup>

$$(\text{cuff, seam}) = (L, M) \xrightarrow{\text{twist}^k} (L, M + kL) \xrightarrow{S^{-1}} (M + kL, L). \quad (25)$$

Hence, the composition of these transformations is given by:  $S^{-1}T^kS$ .

In the previous discussion, we have shown that with two tilted interferometry measurements, we can accomplish the same thing as a double Dehn twist, as far as Chern-Simons theory is concerned, with the caveat that extra Wilson loops might be added to the final state.

One important difference between the Bravyi-Kitaev protocol,<sup>22</sup> and our proposal to mimic this with time-dependent planar topologies is that, in the latter case,  $W(B_1)$  cannot be measured until the end of the entire operation. Consequently, we must use the overpass without knowing if  $W(B_1) = 1$  or  $\psi$  (these are the only two possibilities since two  $\sigma$ 's can only fuse into these two possibilities). This means that we must learn to live with the possibility that  $W(B_1) = \psi$ . The saving grace is that we will at least know after the operation whether  $W(B_1) = 1$  or  $\psi$ , which allows us to compensate in the latter case. Under the assumption that  $W(B_1) = 1$ , we deduced from the  $S$  matrix of the theory that  $W(C)$  is perfectly correlated with  $W(B_0)$ , which is the value of the qubit,

$$W(B_0) = 1 \Rightarrow W(C) = (1 - \psi)/\sqrt{2},$$

$$W(B_0) = \psi \Rightarrow W(C) = \sigma. \quad (26)$$

However, the same logic shows that if  $W(B_1) = \psi$ , then

$$W(B_0) = 1 \Rightarrow W(C) = \sigma,$$

$$W(B_0) = \psi \Rightarrow W(C) = (1 - \psi)/\sqrt{2}. \quad (27)$$

In other words, the correlation between  $W(C)$  and  $W(B_0)$  has been reversed or, in other words, the roles of the states 1 and  $\psi$  of the qubit have been reversed.

In the case of  $g_2$ , this applies to the control qubit, on which all of the operations are performed (the controlled

qubit is passive). Hence, if we find at the end of our procedure that  $W(B_1) = 1$ , then we know that we have applied the desired phase gate  $g_2$ . If, instead,  $W(B_1) = \psi$ , then the gate has inadvertently interchanged the roles of 1 and  $\psi$  within the controlling qubit so that

$$\tilde{g}_2 = \begin{pmatrix} 1 & 0 & 0 & 0 \\ 0 & -1 & 0 & 0 \\ 0 & 0 & 1 & 0 \\ 0 & 0 & 0 & 1 \end{pmatrix}, \quad (28)$$

has instead been applied. This is not too serious since a repeated application of the protocol gives a random walk in the group  $Z_2 \oplus Z_2 = \{1, g_2, \tilde{g}_2, g_2\tilde{g}_2\}$ . Our  $W(B_1)$  measurements tell us where we are within  $Z_2 \oplus Z_2$  as we randomly walk; we simply halt upon reaching  $g_2$ . The tails on a ‘‘long walk’’ decay exponentially so this delay is acceptable.

Now consider  $g_1$ . Let us first suppose, for simplicity, that  $W(\zeta_1) = W(\zeta_2) = 1$ . If we find at the end of our procedure that  $W(B_1) = 1$ , then we know that we have applied  $g_1 = \begin{pmatrix} 1 & 0 \\ 0 & e^{i\pi/4} \end{pmatrix}$ . However, if we find that  $W(B_1) = \psi$ , then we have applied

$$\begin{pmatrix} e^{i\pi/4} & 0 \\ 0 & 1 \end{pmatrix} = e^{i\pi/4} g_1^{-1}. \quad (29)$$

There is one added complication in the case of  $g_1$ , as compared to  $g_2$ : we have the added uncertainty in the outcome of the  $W(\zeta_1)$ ,  $W(\zeta_2)$  measurements. If  $W(\zeta_1) = W(\zeta_2) = \psi$ , then two Wilson loops carrying  $\psi$  appear within the solid torus. However, these two Wilson loops fuse to form 1, which is again trivial, just as in the case  $W(\zeta_1) = W(\zeta_2) = 1$ . However, if  $W(\zeta_1) \cdot W(\zeta_2) = \psi$ , which is as good as a single Wilson loop  $\zeta$  carrying topological charge  $\psi$  parallel to  $C$ , there can be a nontrivial effect. If  $W(C) = (1 - \psi)/\sqrt{2}$ , which means that  $W(B_0) \cdot W(B_1) = 1$ , the Wilson loop contributes no extra phase. However, if  $W(C) = \sigma$ , which means that  $W(B_0) \cdot W(B_1) = \psi$ , then the Wilson loop  $\zeta$  encircles the same topological charge  $\sigma$  that is encircled by  $C$  (to which it is parallel). When a  $\psi$  encircles a  $\sigma$ , a  $(-1)$  results. This means that if  $W(\zeta_1) \cdot W(\zeta_2) = \psi$ , then instead of  $g_1$  or  $g_1^{-1}$ , we have actually applied  $\sigma_z g_1 = g_1^{-3}$  or  $\sigma_z g_1^{-1} = g_1^3$ , where  $\sigma_z = \begin{pmatrix} 1 & 0 \\ 0 & -1 \end{pmatrix}$ .

In all eight measurement outcomes for  $W(\zeta_1)$ ,  $W(\zeta_2)$  we have, up to an overall phase, implemented either  $g_1$ ,  $g_1^{-1}$ ,  $g_1^{-3}$ , or  $g_1^3$ . Thus our protocol generates a type of random walk on  $Z_8$ . Since we know the measurement outcomes we may iterate the protocol until we arrive at  $g_1$ , which is again efficient.

Therefore, we conclude that finding  $W(B_1) = \psi$  is not a calamity for the implementation of either  $g_1$  or  $g_2$ .

### VIII. REALIZING THE BRAVYI-KITAEV GATES WITH TIME-DEPENDENT PLANAR TOPOLOGY AND TILTED INTERFEROMETRY

In this section, we will discuss how the operations of the previous section, which are merely difficult, rather than impossible, might be implemented in a quantum Hall device. We need to be able to do four things: (1) move our qubits at will, (2) create ‘‘faux passes’’—which are equivalent to over-

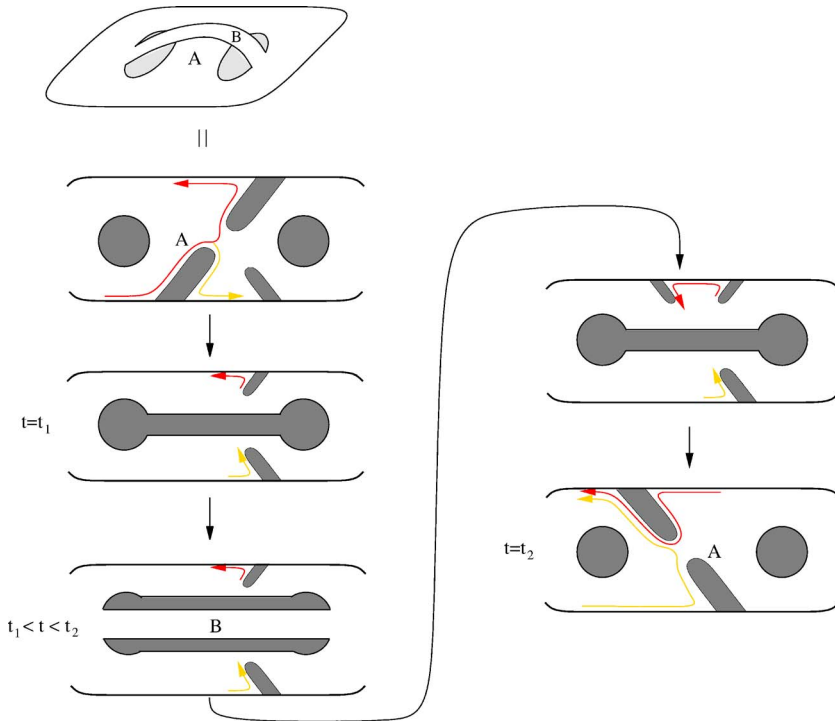


FIG. 20. (Color online) A non-planar overpass configuration can be mimicked by breaking the region  $A$  and adding  $B$ . This is done by merging the two antidots at time  $t_1$  and splitting them in the other direction. The faux pass  $B$  is then used to either apply  $g_1$  or  $g_2$ , as described in Sec. VII. These changes are then undone to return the system to its initial configuration. In order to verify that removing  $A$  was harmless, we have to perform a tilted interferometry measurement in which the red and yellow trajectories interfere.

passes in Chern-Simons theory—with the spacetime histories depicted in Fig. 16 or Fig. 17, (3) measure the topological charge around a tilted trajectory such as  $C$  in Fig. 17, and (4) create a quasiparticle pair and move them around as desired before annihilating them. We have already discussed (1) and (3) in Sec. III. We now turn to (2) and (4).

The spacetime history shown in Fig. 16 can be realized by the sequence of steps depicted in Fig. 20. In this figure, the region  $A$  (the “underpass”) of the quantum Hall fluid separates the two antidots. At time  $t_1$ , region  $A$  is broken so that the two antidots are joined into one large oblong antidot. After this occurs, a strip of quantum Hall fluid is allowed to split the large antidot in the perpendicular direction (the bottom left picture in Fig. 20). This is the faux pass  $B$  that plays the role of the overpass. The spacetime region carved out by this strip is the tube in Fig. 16.

In order to check that the topological charge around the timelike hole is trivial, we need to do a tilted interferometry measurement similar to that depicted in Figs. 9 and 10. The interference between the red and yellow curves in Fig. 20 measures the topological charge around the hole in  $A$ . There is an obvious drawback here, which is that the result of this measurement will not be known until after the entire procedure is complete. We will return to this issue later. For now, let us consider the other operations that we need to perform.

During the time that the faux pass region  $B$  is available, we must take our qubit over it and then check whether the topological charge around the curve  $B_1$  is 1 or  $\psi$ . These are both depicted in Fig. 21. Both of these processes must occur while those depicted in Fig. 20 are simultaneously occurring. We envision doing both of these with a bucket brigade of antidots that are used to ferry both the measuring test quasiparticles and the controlled qubit across the faux pass, as shown in Fig. 22. This is relatively straightforward for the qubit: the two quasiparticles comprising the qubit must be

moved across the region  $B$  in Fig. 20. Of course, this process must occur without the two quasiparticles of the controlled qubit fusing. Hence, we need to keep them far apart, either with a large faux pass or by having one follow at a distance behind the other.

The test quasiparticle with which we measure  $B_1$  is trickier. Consider the red and yellow trajectories in Fig. 21. There should be some small amplitude  $t_r$  for a quasiparticle at the bottom edge to tunnel to the top edge via the red

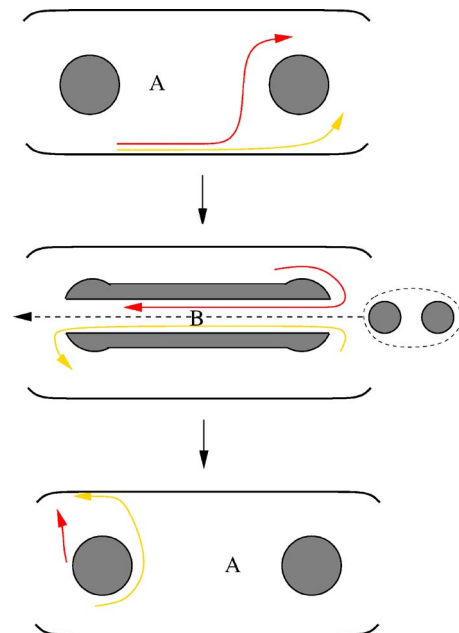


FIG. 21. (Color online) The interference between the red and yellow trajectories is a measurement of the topological charge around  $B_1$ . In order to apply  $g_2$ , we take the controlled qubit across the faux pass.

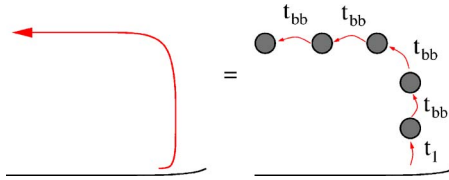


FIG. 22. (Color online) The quasiparticle trajectories shown in Figs. 20 and 21 may actually look more like the trajectory on the right above: a series of hops from one small antidot to another.

trajectory, which takes it over the faux pass, and a small amplitude  $t_y$  for it to tunnel via the yellow trajectory. In the ‘bucket brigade’ scenario, the red trajectory is actually composed of a series of hops from one antidot to another. Let us assume that the amplitude for a quasiparticle to hop from the edge onto the first antidot is  $t_1$ . Let us further assume that the amplitude for it to hop from the first antidot to the second antidot is  $t_{bb}$ ; from the second to the third, again  $t_{bb}$ ; and so on, until the quasiparticle finally hops onto the top edge. Then  $t_r \sim t_1 t_{bb} t_{bb} \dots t_{bb}$ , where the number of factors of  $t_{bb}$  depends on how many antidots are in the bucket brigade. We need this amplitude to be small so that the topological order of the state is not degraded, but it should be large enough to be measurable. This might be most easily done by making  $t_1$  small and  $t_{bb}$  not too small. Of course, the same reasoning holds for the yellow trajectory. Finally, we need the amplitudes for these two processes to interfere coherently. This means that the coherence time for a quasiparticle on either one of these trajectories must be longer than the time of flight, which might be difficult to ensure.

In order to implement  $g_1$ , we need to also send an auxiliary quasiparticle over the faux pass. This can be done, as shown in Fig. 23, perhaps using a ‘bucket brigade,’ as in Fig. 22. We must then measure the topological charge around the curve  $(\zeta_1, -1)$ , which means that we must measure the interference between the trajectories in Fig. 23. We do this with  $(\zeta_2, -1)$  in the same way.

There is a problem with the procedure described in these figures, which is that the configuration shown in the third picture in Fig. 20 has two antidots merged. Consequently, the state of the two antidots does not have exponential protection. The splitting between the two states of the qubit formed by this pair of antidots is  $w \sim 1/x$ , where  $x$  is the linear extent of the merged antidot. This can actually be avoided in the following way. Instead of merging the two antidots, we send an intermediary which shuttles from one to the other. This is done by breaking the antidot on the right into two antidots: one with electrical charge  $e/4$  and the other with no electrical charge. We then move the neutral antidot to the left and merge it with the left antidot. This would simply replace the merger by the ‘tilted merger’ shown in Fig. 17. In order to have an overpass, we need the antidot to be annular so that there is a region of  $\nu = \frac{5}{2}$  quantum Hall fluid in the middle of it, as shown in Fig. 24. While this moving shuttle is between the two antidots, we check by ordinary interferometry that it carries topological charge 1, rather than  $\psi$ . If it does not, then we remerge it with the right antidot and repeat the same process until we find that the topological charge around the shuttle is 1. The abortive attempts at this do not affect the

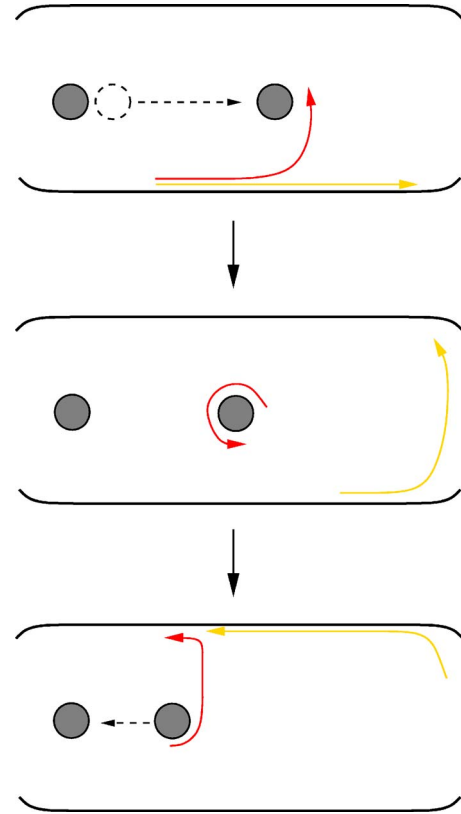


FIG. 23. (Color online) In order to apply  $g_1$ , we must create a pair of auxiliary quasiparticles, take one over the faux pass (not shown), and then annihilate them again. While this is occurring, we must measure the topological charge around a curve that follows the auxiliary quasiparticle over the faux pass, while encircling it. By encircling the auxiliary quasiparticle (presumably while hopping along a bucket brigade of antidots), this trajectory obtains a non-trivial framing: it is the framed curve  $(\xi_i, -1)$ . A measurement of the interference between the red and yellow curves can determine the topological charge around this (tilted) framed curve.

qubit (except possibly by an irrelevant overall phase): splitting  $a$  into  $b \otimes c$  and then refusing results in the original particle type, so it is a multiple of the identity. The qubit is clearly unaffected since the phase resulting from such operations is independent, by locality, of the state of the qubit. In order to apply  $g_2$ , the controlled qubit must sit in the interior of the shuttle as it moves from one antidot of the control qubit to the other. In order to apply  $g_1$ , the auxiliary quasiparticles must do so. It must be noted that this approach again has the difficulty that the coherence times of complicated interfering quasiparticle trajectories must be kept long.

IX. DISCUSSION

In this paper, we have discussed how the  $\nu = 5/2$  quantized Hall plateau can be used as the basis of a quantum computer, assuming that this plateau is in the universality class of the Pfaffian state. Pairs of charge  $e/4$  quasiparticles form qubits. We propose to pin the quasiparticles at antidots so that by moving the antidots, we move the quasiparticles. The two states of a pair of quasiparticles,  $|0\rangle$  and  $|1\rangle$ , can be

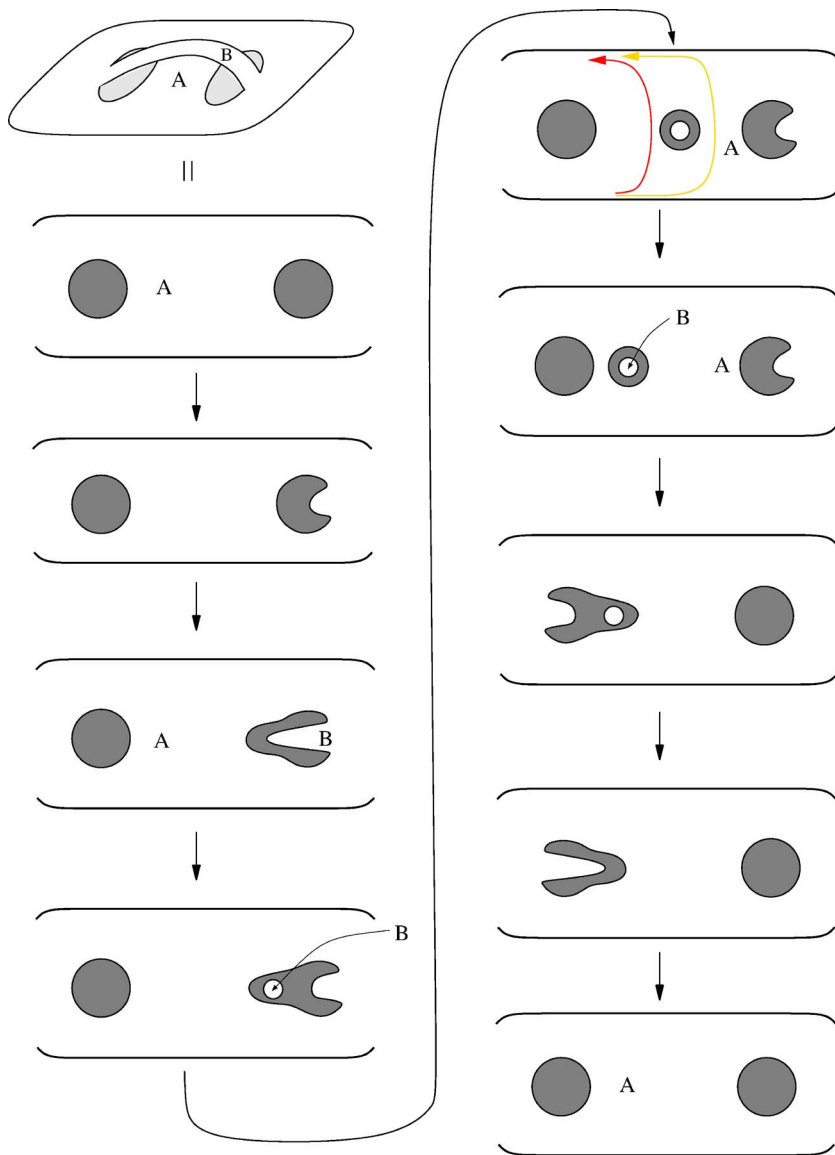


FIG. 24. (Color online) By sending an annular intermediary between the two antidots, we can construct the spacetime history of Fig. 17. The shuttle between the two antidots is annular and the island of quantum Hall fluid in the middle of the annulus is the faux pass  $B$ . A measurement of the interference between the red and yellow trajectories can check that the tilted hole in region  $A$  is topologically trivial as far as Chern-Simons theory is concerned.

identified with the primary fields  $1, \psi$  of the conformal field theory of the critical 2-D Ising model, or with the spin 0 and spin 1 representations of  $SU(2)_2$  Kac-Moody algebra (or the related quantum group). The value of any qubit can be read by a transport measurement that is sensitive to the interference between two possible quasiparticle trajectories encircling the qubit. However, local measurements cannot distinguish the two states of the qubit as long as the two quasiparticles are kept apart. The error rate is astronomically low, so these qubits form an essentially perfect quantum memory.<sup>19</sup> Two simple gates can be implemented by quasiparticle braiding: (1) tunneling a quasiparticle from the edge between the two quasiparticles comprising a qubit and (2) by exchanging a quasiparticle from one qubit with a quasiparticle from another qubit.

In order to be able to apply any possible unitary transformation to our qubits—i.e., in order to have a universal quantum computation—we can try either of two approaches. One is to use the unprotected operation of bringing together the two quasiparticles comprising a qubit so that a phase gate will result from the resulting energy splitting between their

two states. Although this operation is unprotected, the error threshold may not be too strict because the other operations are exact due to topological protection. The other approach is to use some complicated manipulations of the antidots that involves moving, splitting, and rejoining them in order to fool the topological field theory governing the Pfaffian state into behaving as if we have performed nonembeddable topology changes. Although complicated, these operations allow, in principle, for a universal set of exact gates. By now the reader may have decided that the former approach is more promising in the short run because it does not require extremely complicated quasiparticle manipulations. However, if technological advances make the latter approach more feasible, then it has the virtue of complete topological protection. Also, the beautiful topology involved lends it an intrinsic “coolness” factor.

If the weaker  $\nu = \frac{12}{5}$  plateau proves to be a non-Abelian state related to  $SU(2)_3$  Chern-Simons theory, then neither of these two compromises would be necessary. We would again realize qubits as previously, but, in this case, the braid group

alone would be sufficient for a universal quantum computation.

*Note added in proofs.* After the completion of this work, we became aware of a preprint by Bravyi,<sup>34</sup> in which precise error correction protocols are given for quantum computation at  $\nu = \frac{5}{2}$  using the unprotected operation of (21) and the two-qubit measurement of Fig. 13. The fault-tolerance thresholds which Bravyi finds for these operations are 14% and 38%, respectively.

### ACKNOWLEDGMENTS

We would like to thank S. Das Sarma, M. P. A. Fisher, A. Kitaev, C. Marcus, K. Shtengel, J. Slingerland, and A. Stern for discussions. We would especially like to thank P. Bonderson for discussions and a careful reading of earlier versions of this paper. We would also like to acknowledge the hospitality of the Kavli Institute for Theoretical Physics at UCSB and the Aspen Center for Physics. We have been supported by the ARO under Grant No. W911NF-04-1-0236. C.N. has also been supported by NSF under Grant No. DMR-0411800.

### APPENDIX A: EFFECTIVE FIELD THEORY APPROACH TO THE PFAFFIAN STATE

The multiqasihole structure that we encountered in Sec. II is precisely the same structure as occurs in the Ising model. Indeed, the motivation of Moore and Read for first writing down the Pfaffian wave function was its relation to conformal blocks of the Ising model.<sup>6</sup> The first hint that there might be such a connection comes from the observation that the Pfaffian factor in the wave function (1) is equal to a correlator of  $\psi$  fields:

$$\langle \psi(z_1)\psi(z_2) \dots \psi(z_{2n}) \rangle = \text{Pf} \left( \frac{1}{z_j - z_k} \right). \quad (\text{A1})$$

Multiquasihole wave functions are related to conformal blocks with spin fields such as Refs. 6 and 8. Before discussing this in any more detail, however, we should first explain why the quasiparticles of the Pfaffian state have anything to do with the primary fields of the Ising model.

The answer lies in the connection discovered by Witten<sup>35</sup> between 2+1D Chern-Simons theories and 1+1- or 2-D conformal field theories (CFTs). According to Witten<sup>35</sup> (see also the explicit constructions of Elitzur *et al.*<sup>36</sup>), the Hilbert space of states of a Chern-Simons theory on a 3-D manifold  $M = X \times R$  is equivalent to the vector space of conformal blocks of an associated CFT on the 2-D manifold  $X$ . The Hilbert space of a Chern-Simons theory with sources located at  $\mathbf{r}_1, \mathbf{r}_2, \dots, \mathbf{r}_n$  carrying representations  $\rho_1, \rho_2, \dots, \rho_n$  is equivalent to the conformal blocks of an  $n$ -point correlation function of primary fields associated with these representations.

If we have an electron system that is described at long wavelengths by a Chern-Simons theory, we can use the wave functions of the Chern-Simons theory with sources as approximate wave functions of the electron system. By the above connection, this means we can use conformal blocks

in the associated CFT as wave functions of the electron system. In each of these two steps, the essential features that are preserved are the braiding properties of the quasiparticles of the system. The different primary fields in the CFT correspond to the different topological charges in the Chern-Simons theory, which, in turn, correspond to the different quasiparticle species in the electron system.

As shown in Refs. 15 and 16 the low-energy effective field theory associated with the Pfaffian state of bosons at  $\nu = 1$  is an  $SU(2)_2$  Chern-Simons theory. The effective field theory for fermions at  $\nu = \frac{1}{2}$  (or other even-denominator filling fractions and for bosons at other odd-denominator filling fractions) is a deformation of this theory: a Higgs-ed  $SU(2)_2$  Chern-Simons theory (independent of the filling fraction) coupled to a  $U(1)$  Chern-Simons theory with a filling-fraction-dependent coupling constant. The CFT corresponding to this Chern-Simons theory is the tensor product of an  $SU(2)/U(1)$  coset model with a  $c=1U(1)$  factor.<sup>6</sup> However, the  $SU(2)/U(1)$  coset model is equivalent to the Ising model. According to this correspondence, the primary fields that are associated with half-flux quantum quasiparticles are Ising spin fields (multiplied by a field from the  $c=1$  sector).

The  $U(1)$  factor, which accounts for the charge, gives the correct Abelian factors for quasiparticle statistics and contributes a factor to the ground state degeneracy. The more nontrivial physics is contained in the  $SU(2)$  part of the theory. Hence, we can be a little sloppy and drop their  $U(1)$  quantum numbers and refer to quasiparticles by their  $SU(2)_2$  quantum numbers (which we will call ‘‘isospin’’). According to this nomenclature, there are three primary fields, with isospins  $0, \frac{1}{2}, 1$ , corresponding to  $1, \sigma, \psi$  of the Ising model. These are, respectively, the vacuum, the half-flux quantum quasiparticle, and the neutral fermion. The topological degeneracy of multiqasihole states reflects the decomposition of the product of two isospin  $1/2$ s:  $\frac{1}{2} \otimes \frac{1}{2} = 0 \oplus 1$ . Thus, there are two different reasons why it is natural to call the two states of a qubit 0 and 1.

Returning now to the conformal blocks that model wave functions of electrons at  $\nu = \frac{1}{2}$  (in the first excited Landau level), we note that the corresponding CFT contains both the  $c=1/2$  Ising model and a  $c=1$  chiral boson (accounting for the electrical charge):

$$S = \int d^2z [\psi \partial_{\bar{z}} \psi + (\partial_z \phi)(\partial_{\bar{z}} \phi)]. \quad (\text{A2})$$

We retain only the right-handed part  $\varphi$  of  $\phi = \varphi + \bar{\varphi}$ , with  $\partial_{\bar{z}} \varphi = \partial_z \bar{\varphi} = 0$ . If we assume that the operator corresponding to the electron is

$$\Psi_{\text{el}}(z) = \psi(z) e^{i\varphi(z)\sqrt{2}}, \quad (\text{A3})$$

then we have

$$\begin{aligned} & \langle \Psi_{\text{el}}(z_1) \Psi_{\text{el}}(z_2) \dots \Psi_{\text{el}}(z_{2N}) e^{i \int d^2z \rho \varphi(z) \sqrt{2}} \rangle \\ &= \prod_{j < k} (z_j - z_k)^2 \prod_j e^{-|z_j|^2/4} \cdot \text{Pf} \left( \frac{1}{z_j - z_k} \right). \end{aligned} \quad (\text{A4})$$

The last term in the correlation function on the left-hand side

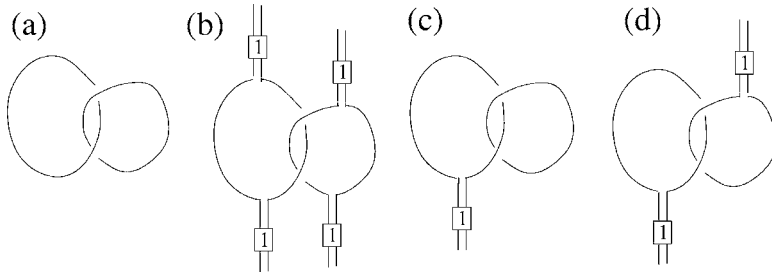


FIG. 25. By evaluating the Jones polynomial at  $q = \exp(\pi i/4)$  for these links, we can obtain the desired matrix elements for braiding operations manipulating the qubit. The boxed 1 is a projector on the pair of quasiparticles that puts them in the state  $|1\rangle$ .

of this equation is a neutralizing charge background without which the Coulomb gas correlation function would vanish. To find the primary fields of this  $c=3/2$  theory, we need to put together the primary fields of the (right-handed chiral component of the) Ising model—the identity (1); the Ising spin field,  $\sigma$ ; and the Majorana fermion,  $\psi$ —with exponentials of the chiral boson  $\varphi$ . The primary fields must be local with respect to the electron operator—i.e., quasiparticles can have nontrivial statistics with each other, but they must have trivial statistics with respect to an electron since an electron wave function must be single valued in electron coordinates. A field that satisfies this condition is

$$\Phi_{\text{qp}}(\eta) = \sigma(\eta) e^{i\varphi(\eta)/2\sqrt{2}}. \quad (\text{A5})$$

This field corresponds to the charge  $e/4$  quasiparticle:

$$\begin{aligned} & \langle \Phi_{\text{qp}}(\eta_1) \Phi_{\text{qp}}(\eta_2) \times \Psi_{\text{el}}(z_1) \Psi_{\text{el}}(z_2) \dots \Psi_{\text{el}}(z_{2N}) e^{\int d^2z \rho \varphi(z) \sqrt{2}} \rangle \\ &= \text{Pf} \left( \frac{(z_j - \eta_1)(z_k - \eta_2) + z_j \leftrightarrow z_k}{z_j - z_k} \right) \\ & \times \prod_{j < k} (z_j - z_k)^2 \prod_j e^{-|z_j|^2/4}. \end{aligned} \quad (\text{A6})$$

The four-quasihole wave functions in (9) are given by the conformal blocks of

$$\langle \Phi_{\text{qp}} \Phi_{\text{qp}} \Phi_{\text{qp}} \Phi_{\text{qp}} \Psi_{\text{el}} \Psi_{\text{el}} \dots \Psi_{\text{el}} \exp(\int d^2z \rho \varphi \sqrt{2}) \rangle.$$

The two different wave functions correspond to the two different fusion channels  $\sigma \cdot \sigma \sim 1 + \psi$ . [Furthermore, the two conformal blocks are the wavefunctions (9) in the special basis in which the explicit monodromy of the wavefunction gives the complete braiding matrices<sup>9</sup>].

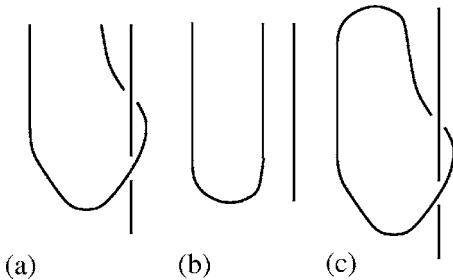


FIG. 26. (a) A quasiparticle trajectory that winds around a quasiparticle at an antidot (b) a quasiparticle trajectory that does not wind around the antidot; (c) the matrix element between the states resulting from these two trajectories.

The full set of primary fields is given in the following table. The columns correspond to Ising model primary fields while the rows correspond to the  $c=1$  primary fields. The entries of the table are the quasiparticle electrical charges. Each quasiparticle corresponds to an operator formed by multiplying the operator at the top of its column by the operator to the left of its row. Note that it is not a naive tensor product between the two theories because the quasiparticles containing  $\sigma$  are offset by  $e^{i\varphi/2\sqrt{2}}$  from those containing 1,  $\psi$ . [Again, these assignments are determined by the requirement of locality with respect to the electron operator (A3).]

	1	$\sigma e^{i\varphi/2\sqrt{2}}$	$\psi$
1	0	$e/4$	0
$e^{i\varphi/\sqrt{2}}$	$e/2$	$3e/4$	$e/2$

One of the nice features of the relationship between the Pfaffian state and  $SU(2)_2$  Chern-Simons theory is that it allows us to use Witten's remarkable result relating Chern-Simons theory and the Jones polynomial of knot theory.<sup>35</sup> Braiding matrix elements can be obtained by computing the Jones polynomial of the corresponding link diagrams.<sup>15,19,28</sup> For instance, the qubit-flipping property of the process that takes  $\eta_3$  around  $\eta_1$  in (9) can be obtained by evaluating the Jones polynomial (operator) at  $q = e^{\pi i/4}$  for the links in Fig. 25.

What do these pictures mean and how are they evaluated? They are essentially Feynman diagrams for the topological interactions of quasiparticles. The lines in this picture represent isospin 1/2 quasiparticles. Since the electric charge is not accounted for in these diagrams, quasiparticles and quasiholes are identical as far as these diagrams are concerned. (The electric charge just contributes Abelian phase factors.) If two of these isospin 1/2 quasiparticles fuse to form a spin 0, then they can annihilate to give the vacuum. Otherwise, they fuse to form an isospin 1 particle, which we denote by a boxed 1 on the two lines (as in Fig. 25(b), for example). Consider, for instance, the spacetime trajectories of the test quasiparticle and the quasiparticle on the antidot in Fig. 7. They will look like Fig. 26(a). In this figure, we assume that a quasiparticle-quasihole pair is created at  $P$  and the quasiparticle goes around the antidot. The other trajectory, with which this interferes, is depicted in Fig. 26(b): in this case, the test quasiparticle does not go around the antidot. The interference term between these two processes, i.e., the third term in Eq. (13), is given by the matrix element between these two processes, depicted in Fig. 26(c). It is just Fig. 26(b) inverted (which corresponds to turning a ket into a bra) and then stacked on top of Fig. 26(a). This matrix ele-

ment measures the topological charge associated with the loop in Fig. 26(c).

Hence, to summarize: we specify an initial state  $|\psi_0\rangle$  of  $n$  qubits by drawing  $2n$  incoming lines, which are grouped into  $n$  pairs. At the bottom of the diagram (the distant past), each pair is either created from the vacuum (in which case this qubit is in the state  $|0\rangle$ ) or was fused to form an isospin 1 particle (in which case this qubit is in the state  $|1\rangle$ ). The final state  $|\psi\rangle$  is obtained by braiding these quasiparticles, which is depicted in the figure with the vertical direction on the page being positive time. Finally, the matrix element between  $|\psi\rangle$  and another state  $|\chi\rangle$  is obtained by inverting the corresponding diagram for  $|\chi\rangle$  and stacking it on top of the diagram for  $|\psi\rangle$ , connecting each quasiparticle line from  $\langle\chi|$  to the corresponding quasiparticle line from  $|\psi\rangle$ .

The matrix element associated with such a diagram is evaluated recursively in the following way. Each diagram is replaced by the sum of two diagrams both of which have one fewer crossing according to the rule

$$\text{Y} = q^{1/2} \text{I} + q^{-1/2} \text{U} \tag{A7}$$

The new diagrams come with corresponding coefficients as indicated in the above relation. We continue this procedure until all crossings are eliminated. The projector on the isospin 1 state is replaced by the explicit expression

$$\text{I} = \text{I} - \frac{1}{d} \text{U} \tag{A8}$$

where  $d = -q - q^{-1}$ . Finally, every closed loop is given the value

$$\text{O} = d \tag{A9}$$

**APPENDIX B: THE EFFECT OF ADDING OR DELETING BANDS OF MATERIAL TO A TOPOLOGICAL STATE**

In this appendix, we discuss how a  $\nu = \frac{5}{2}$  fractional quantum Hall droplet is modified by topology change, in particular when bands of material are added or deleted. The basic guideline is that adding a band of material does not change the state of the system, so it is reversible; deleting a band of material can cause the state of the system to change irreversibly.

In the Bravyi-Kitaev construction discussed in section VI, we described a process in which a band of material (the overpass in the middle picture in Fig. 15) is added and then later removed. The spacetime history of such a process is depicted in Fig. 27. In this figure, two  $\sigma$  quasiparticles on antidots fuse to form 1 or  $\psi$ , which is the topological charge of the boundary. The spacetime history of the quantum Hall droplet with two antidots is shown as a “pair of pants” legs  $P \times I$ , where  $P$  is the disk with two punctures and  $I$  is the interval of time  $[0,1]$ . The spacetime history depicting the addition and subsequent removal of an overpass connecting

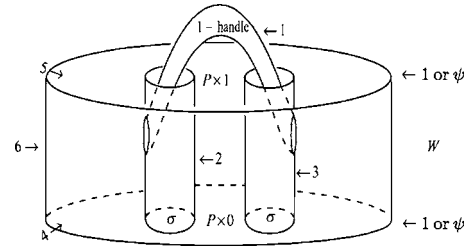


FIG. 27. The spacetime history of a process in which an overpass connecting two antidots is added and then removed. Warning: this history does not embed in 2+1 dimensions, so the  $z$  coordinate in this picture cannot be literally interpreted as time. The handle must move into a fourth direction.

the antidots is a handle connecting the two pants legs. The union of this 1-handle and the spacetime history of the droplet with two antidots is  $W = P \times I \cup$  (1-handle).

We would like to check that this procedure leaves invariant the qubit supported by  $P$  (rather than, say, applies a phase gate). In order to do this, we imagine evaluating the Chern-Simons functional integral on the 3-manifold  $W$ . It will give a state in the Hilbert space of the boundary  $\partial W$ . However, this boundary is divided into subsurfaces by loops bounding specified topological charges, so the Hilbert space of the boundary is, in fact, the tensor product of the Hilbert spaces of the subsurfaces. Hence,  $W$  specifies a vector  $\psi_1$  in:  $V_{0,0} \otimes V_{0,\sigma,\sigma} \otimes V_{0,\sigma,\sigma} \otimes V_{\sigma,\sigma,x} \otimes V_{\sigma,\sigma,x}^* \otimes V_{x,x}$ , where the factors come from subsurfaces 1,...,6 in Fig. 22. The zero label in the first three factors is dictated by the presence of disks in  $W$  capping the boundary of the first component (a cylinder). The gluing axiom<sup>33,37</sup> tells us that removing the 1-handle determines a canonical isomorphism to  $Z(P \times I)$  carrying  $\psi_1$  to  $\psi_0$  in  $V_0^* \otimes V_0 \otimes V_{0,\sigma,\sigma} \otimes V_{0,\sigma,\sigma} \otimes V_{\sigma,\sigma,x} \otimes V_{\sigma,\sigma,x}^* \otimes V_{x,x}$ . After supplying the canonical base vectors  $\beta_0 \in V_0^*, \beta_{0,\sigma,\sigma} \in V_{0,\sigma,\sigma}$  and  $\beta_{x,x} \in V_{x,x}$ ,  $\psi_1$  is canonically identified with  $\text{id} \in \text{Hom}(V_{\sigma,\sigma,x}) \cong V_{\sigma,\sigma,x}^* \otimes V_{\sigma,\sigma,x}$ . Note that no  $x$ -dependent phase has entered the calculation. Thus we have proved, in the abstract language of TQFTs, that adding and then breaking a band induces the identity operator on the qubit supported in  $P$ .

The situation is rather different if, instead, we cut out a band to join the internal punctures and then restore it (i.e., fuse the internal punctures and then separate them). This is true regardless of whether we assume that we can use the electric charge of the  $\sigma$ s to ensure that each resulting punc-

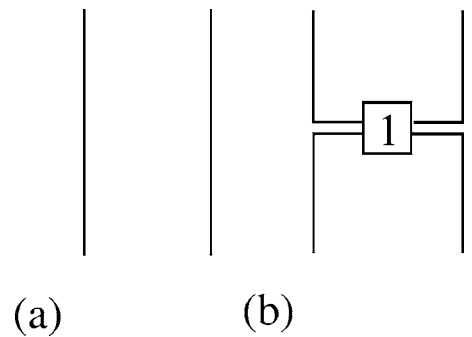


FIG. 28. The spacetime history of Fig. 27 is equivalent to the Feynman diagrams above in the notation introduced in Appendix A.

ture again carries a charge- $\frac{e}{4}\sigma$  after they are fused and split. Such an operation is depicted in Fig. 9. We show below that this operation acts on  $P$  by the identity if  $\gamma$  has topological charge 1. If it has topological charge  $\psi$ , however, it is  $\sigma_z$ . If it is a linear superposition of these two possibilities, then the applied gate is the same linear combination of 1 and  $\sigma_z$ . The moral, in general, is that operations which add quantum media (in this case,  $\nu=\frac{5}{2}$ —FQHE fluid) are reversible—simply delete what was previously added, whereas operations that delete are often irreversible.

This operation can be depicted in the Feynman diagram notation introduced in appendix A. It is either Figs. 28(a) or

28(b), according to the charge of  $\gamma$ .

Clearly, both operators are diagonal in the  $(1, \psi)$  basis. Furthermore, Fig. 28(a) is simply the identity acting on the  $P$  qubit. This may be verified by direct computation of the diagonal entries. Using the rules introduced in Appendix A, we  $\sqrt{2}\cdot 1$ . The strange  $\sqrt{2}$  factor is actually  $S_{11}=S_{\psi\psi}$  that has entered because we have not rescaled the dual physical Hilbert space by  $1/S_{11}$  prior to gluing. Taking this factor into account, we obtain the identity.

Computing the diagonal entries for the second process, we obtain  $\sigma_z$ , as claimed, after taking into account the correction described above and rescaling by  $1/S_{\psi\psi}$ .

- 
- <sup>1</sup>A related paper, cond-mat/0512072, explains the topological issues in greater detail. It may help the reader to look at this alternate presentation if confused about any point.
- <sup>2</sup>See, for instance, *Perspectives in Quantum Hall Effects: Novel Quantum Liquids in Low-Dimensional Semiconductor Structures*, edited by S. Das Sarma and A. Pinczuk (Wiley, New York, 1997), and references therein.
- <sup>3</sup>J. Leinaas and J. Myrheim, *Nuovo Cimento Soc. Ital. Fis.*, **B 37B**, 1 (1977); G. Goldin *et al.*, *J. Math. Phys.* **22**, 1664 (1981); F. Wilczek, *Phys. Rev. Lett.* **48**, 1144 (1982). See also the discussion in *Fractional Statistics and Anyon Superconductivity*, edited by F. Wilczek (World Scientific, Singapore, 1990).
- <sup>4</sup>However, direct experimental verification of this has proven difficult until now; see F. E. Camino, W. Zhou, and V. J. Goldman, cond-mat/0502406.
- <sup>5</sup>J. S. Xia, W. Pan, C. L. Vicente, E. D. Adams, N. S. Sullivan, H. L. Stormer, D. C. Tsui, L. N. Pfeiffer, K. W. Baldwin, and K. W. West, *Phys. Rev. Lett.* **93**, 176809 (2004); J. P. Eisenstein, K. B. Cooper, L. N. Pfeiffer, and K. W. West, *ibid.* **88**, 076801 (2002); W. Pan, J. S. Xia, V. Shvarts, D. E. Adams, H. L. Stormer, D. C. Tsui, L. N. Pfeiffer, K. W. Baldwin, and K. W. West, *Phys. Rev. Lett.* **83**, 3530 (1999); J. P. Eisenstein *et al.*, *Surf. Sci.* **229**, 31 (1990); R. L. Willett, J. P. Eisenstein, H. L. Stormer, D. C. Tsui, A. C. Gossard, and J. H. English, *Phys. Rev. Lett.* **59**, 1776 (1987).
- <sup>6</sup>G. Moore and N. Read, *Nucl. Phys. B* **360**, 362 (1991).
- <sup>7</sup>M. Greiter, X.-G. Wen, and F. Wilczek, *Nucl. Phys. B* **374**, 567 (1992).
- <sup>8</sup>I. C. Nayak and F. Wilczek, *Nucl. Phys. B* **479**, 529 (1996).
- <sup>9</sup>V. Gurarie and C. Nayak, *Nucl. Phys. B* **506**, 685 (1997).
- <sup>10</sup>Y. Tserkovnyak and S. H. Simon, *Phys. Rev. Lett.* **90**, 016802 (2003).
- <sup>11</sup>N. Read and E. Rezayi, *Phys. Rev. B* **54**, 16864 (1996).
- <sup>12</sup>N. Read and D. Green, *Phys. Rev. B* **61**, 10267 (2000).
- <sup>13</sup>D. A. Ivanov, *Phys. Rev. Lett.* **86**, 268 (2001).
- <sup>14</sup>A. Stern, F. von Oppen, and E. Mariani, *Phys. Rev. B* **70**, 205338 (2004).
- <sup>15</sup>E. Fradkin, C. Nayak, A. M. Tsvelik, and F. Wilczek, *Nucl. Phys. B* **516**, 704 (1998).
- <sup>16</sup>E. Fradkin, C. Nayak, and K. Schoutens, *Nucl. Phys. B* **546**, 711 (1999).
- <sup>17</sup>R. H. Morf, *Phys. Rev. Lett.* **80**, 1505 (1998).
- <sup>18</sup>E. H. Rezayi and F. D. M. Haldane, *Phys. Rev. Lett.* **84**, 4685 (2000).
- <sup>19</sup>S. Das Sarma, M. Freedman, and C. Nayak, *Phys. Rev. Lett.* **94**, 166802 (2005).
- <sup>20</sup>A. Y. Kitaev, *Ann. Phys.* **303**, 2 (2003).
- <sup>21</sup>M. H. Freedman, A. Kitaev, M. Larsen, and Z. Wang, quant-ph/0101025.
- <sup>22</sup>S. Bravyi and A. Yu. Kitaev, “Quantum invariants of 3-manifolds and quantum computation,” 2001 preprint.
- <sup>23</sup>N. Read and E. Rezayi, *Phys. Rev. B* **59**, 8084 (1999).
- <sup>24</sup>M. Freedman, M. Larsen, and Z. Wang, *Commun. Math. Phys.* **227**, 605 (2002).
- <sup>25</sup>It is easier to write down explicit wavefunctions for quasiholes than for quasiparticles, so we restrict attention in this section to quasiholes. For the particular device configurations that we discuss in this paper, it is also easier to work with quasiholes. However, the underlying topological properties are the same, so we will use the terms “quasiparticle” and “quasihole” almost interchangeably.
- <sup>26</sup>C. de C. Chamon, D. E. Freed, S. A. Kivelson, S. L. Sondhi, and X. G. Wen, *Phys. Rev. B* **55**, 2331 (1997).
- <sup>27</sup>A. Stern and B. I. Halperin, cond-mat/0508447.
- <sup>28</sup>P. Bonderson, A. Kitaev, and K. Shtengel, *Phys. Rev. Lett.* **96**, 016803 (2006).
- <sup>29</sup>Y. Aharonov and D. Bohm, *Phys. Rev.* **115**, 485 (1959).
- <sup>30</sup>Presumably it is controlled by variable-range hopping at still lower temperatures. In this regime, a quasiparticle which is in one localized state at zero temperature is thermally excited into another localized state. Through a sequence of such hops, with an average range which varies with temperature, it travels across the system.
- <sup>31</sup>S. Bravyi and A. Kitaev, *Ann. Phys.* **298**, 210 (2002).
- <sup>32</sup>S. Bravyi and A. Kitaev, *Phys. Rev. A* **71**, 022316 (2005).
- <sup>33</sup>K. Walker, “On Witten’s 3-manifold invariants,” preprint, 1991 (available at <http://canyon23.net/math/>).
- <sup>34</sup>S. Bravyi, quant-ph/0511178.
- <sup>35</sup>E. Witten, *Commun. Math. Phys.* **121**, 351 (1989).
- <sup>36</sup>S. Elitzur, G. Moore, A. Schwimmer, and N. Seiberg, *Nucl. Phys. B* **326**, 108 (1989).
- <sup>37</sup>V. Turaev, *Introduction to Combinatorial Torsions*, 1st ed. (Birkhauser, Basel, 2000).